Exploring the Scalability Limits of Communication Networks at the Nanoscale

Thesis submitted in partial fulfillment of the requirements for the degree of
Master in Computer Architecture, Networks and Systems

by

Ignacio Llatser Martí

Advisors:
Dr. Eduard Alarcón Cot
Dr. Albert Cabellos-Aparicio

2011

Nanonetworking Center in Catalunya (N3Cat)
Universitat Politècnica de Catalunya

Abstract

Nanonetworks, the interconnection of nanomachines, will greatly expand the range of applications of nanotechnology, bringing new opportunities in diverse fields. Following preliminary studies, two paradigms that promise the realization of nanonetworks have emerged: molecular communication and nano-electromagnetic communication.

In this thesis, we study the scalability of communication networks when their size shrinks to the nanoscale. In particular, we aim to analyze how the performance metrics of nanonetworks, such as the channel attenuation or the propagation delay, scale as the size of the network is reduced.

In the case of nano-electromagnetic communication, we focus on the scalability of the channel capacity. Our quantitative results show that due to quantum effects appearing at the nanoscale, the transmission range of nanomachines is higher than expected. Based on these results, we derive guidelines regarding *how* network parameters, such as the transmitted power, need to scale in order to keep the network feasible.

In molecular communication, we concentrate in a scenario of short-range molecular signaling governed by Fick's laws of diffusion. We characterize its physical channel and we derive analytical expressions for some key performance metrics from the communication standpoint, which are validated by means of simulation. We also show the differences in the scalability of the obtained metrics with respect to their equivalent in wireless electromagnetic communication.

Finally, we have designed *NanoSim*, a physical simulation framework for diffusion-based molecular communication. We think that *NanoSim* will prove an essential tool to design and evaluate protocols, modulations, resource management schemes and a novel network architecture for molecular nanonetworks.

We consider that the results of this thesis provide interesting insights which may serve designers as a guide to implement future nanonetworks, and lay the foundations of a scalability theory for nanonetworks.

Acknowledgements

First and foremost I would like to express my deep and sincere gratitude to professors Eduard Alarcón Cot and Albert Cabellos-Aparicio, who jointly supervised this master thesis. Their invaluable insights and guidance have been a source of inspiration throughout the development of this project. Most of the ideas contained in this work originated in the stimulating discussions that we held together.

I am also very grateful to Prof. Josep Solé-Pareta for giving me the opportunity to join the Nanonetworking Center in Catalunya, and to Prof. Ian F. Akyildiz for his expert advice at crucial stages of the project. I greatly appreciate as well the financial support offered by the FPI grant from the Technical University of Catalonia and the FPU grant from the Spanish Ministry of Education for the development of this thesis.

I would also like to take this opportunity to acknowledge my colleagues at the Nanonetworking Center in Catalunya. Special thanks go to Iñaki Pascual, Nora Garralda, Maria Gregori, Massimiliano Pierobon and Josep Miquel Jornet for their excellent work and tireless dedication. Their valuable comments have undoubtedly helped to improve this thesis.

Last but certainly not least, a big thank you goes to my parents, my brother Franc and the rest of my family for their unconditional support throughout my life.

Contents

1 Introduction **1**
- 1.1 Nanotechnology . . . 1
- 1.2 Nanonetworks . . . 2
  - 1.2.1 Molecular Communication . . . 2
  - 1.2.2 Nano-electromagnetic Communication . . . 3
- 1.3 Applications of Nanonetworks . . . 6
- 1.4 Motivation of this Thesis . . . 7
- 1.5 Main Contributions . . . 8

2 Scalability of the Channel Capacity of Electromagnetic Nanonetworks **10**
- 2.1 Introduction . . . 10
- 2.2 Electromagnetic Communication at the Nanoscale . . . 11
  - 2.2.1 Nano-electromagnetic Physical Channel Model . . . 11
  - 2.2.2 Quantum Effects . . . 14
  - 2.2.3 Bandwidth and Channel Capacity . . . 16
- 2.3 Nano-electromagnetic Channel Capacity . . . 16
  - 2.3.1 Channel Bandwidth . . . 18
  - 2.3.2 Transmitted Power Spectral Density . . . 19
  - 2.3.3 Channel Attenuation . . . 19
  - 2.3.4 Noise Power Spectral Density . . . 19
  - 2.3.5 Expression of the Channel Capacity . . . 20
  - 2.3.6 Quantitative Results . . . 21
- 2.4 Limits of the Channel Capacity . . . 23
- 2.5 Scalability guidelines . . . 24

3 Diffusion-based Channel Characterization in Molecular Nanonetworks **27**
- 3.1 Introduction . . . 27
- 3.2 Diffusion-based Molecular Channel and Modulation Scheme . . . 28
- 3.3 Molecular Channel Analysis . . . 29
- 3.4 Communication Metrics . . . 31
  - 3.4.1 Pulse Delay . . . 31
  - 3.4.2 Pulse Amplitude . . . 32
  - 3.4.3 Pulse Width . . . 33
  - 3.4.4 Molecular vs Wireless EM Channel Comparison . . . 34

3.5 Achievable Bandwidth 35
3.6 Multiple Transmitters 36

4 NanoSim: A Simulation Framework for Diffusion-based Molecular Communication 38
4.1 Introduction 38
4.2 Simulator Architecture 39
4.2.1 Transmitter and Receiver Models 39
4.2.2 Particle Model 40
4.2.3 Simulation Space 40
4.3 Simulation Results 41

5 Conclusions and future work 44
5.1 Conclusions 44
5.2 Future work 45

A Derived publications and theses 47
A.1 Publications derived from this thesis 47
A.2 Supervised master theses 47

List of Figures

1.1 Conceptual diagram of a nanomachine in the electromagnetic domain [6]. 2
1.2 Short range molecular communication techniques: molecular signaling (top) and molecular motors (bottom) [4]. 4
1.3 Medium range molecular communication techniques: flagellated bacteria (top) and catalytic nanomotors (bottom) [30, 31]. . . . 5
1.4 Long range molecular communication techniques: axons (top) and light transduction (bottom) [47]. 5
1.5 Idealized structure of a single graphene sheet. 6
1.6 Applications of nanonetworks: intrabody nanonetworks for healthcare applications (left) and the interconnected office (right) [5]. . 7

2.1 Total path loss in dB as a function of frequency f and distance d in a standard medium with 10% of water vapor molecules (the values for path loss have been truncated at 120 dB to avoid masking relevant transmission windows in the short-range). . . . 13
2.2 Noise temperature as a function of frequency f and distance d in a standard medium with 10% of water vapor molecules. . . . 14
2.3 Log-log plot of the wave propagation speed as a function of the antenna width W, without quantum effects ($v_{p_{nq}}$, blue solid line) and with quantum effects (v_{p_q}, red dashed line). 15
2.4 Quantitative values of the channel capacity C as a function of the nanomachine size Δ and the transmission distance d, without quantum effects. 22
2.5 Quantitative values of the channel capacity C as a function of the nanomachine size Δ and the transmission distance d, with quantum effects. 22
2.6 Feasible area of the channel capacity as a function of α and β. The blue solid line corresponds to the case when quantum effects are not present, and the red dashed line when they are. . 25
2.7 Log-log plot comparing the scalability of the transmitted power without quantum effects ($P_{T_{nq}}$, blue solid line) and with quantum effects (P_{T_q}, red dashed line), as a function of the nanomachine size Δ. The transmission distance scales as $d = \Theta(\Delta)$. . . 26

3.1 Normalized channel impulse response. 29

3.2 Magnitude of the normalized channel transfer function in dB. . 30
3.3 Channel group delay. 30
3.4 Magnitude of the normalized channel transfer function in dB as a function of the transmission distance. 31
3.5 Channel group delay as a function of the transmission distance. 32
3.6 Plot of the pulse delay as a function of the transmission distance. The dashed line corresponds to the analytical expression, and the crosses show the simulation results with 95% confidence intervals. 33
3.7 Log-log plot of the pulse amplitude as a function of the transmission distance. The dashed line corresponds to the analytical expression, and the crosses show the simulation results with 95% confidence intervals. 34
3.8 Plot of the pulse width as a function of the transmission distance. The dashed line corresponds to the analytical expression, and the crosses show the simulation results with 95% confidence intervals. 35
3.9 Concentration measured by the receiver when a train of pulses is transmitted from a distance of 200 nm. The interval between pulses is equal to the pulse width at the receiver location. 36
3.10 Concentration measured by the receiver when two transmitters simultaneously emit a molecular pulse. Transmitter 1 (orange) is located at a distance of 300 nm, and transmitter 2 (blue) at 400 nm. 37

4.1 Block diagram of *NanoSim* 39
4.2 Transmission of a Gaussian pulse 42
4.3 Transmission of a square pulse 43

Chapter 1

Introduction

1.1 Nanotechnology

Nanotechnology, first envisioned by the Nobel laureate physicist Richard Feynman in his famous speech entitled "There's plenty of room at the bottom" in 1959, is giving rise to devices in a scale ranging from one to a few hundred nanometers. During the last few decades, emerging research areas such as nanoelectronics, nanomechanics and nanophotonics are allowing the development of novel nanomaterials, nanocrystals, nanotubes and nanosystems that promise to revolutionize many fields of science and engineering.

Molecular nanotechnology, popularized by Eric Drexler [19], is a technology based on the ability to build molecular machines by means of mechanosynthesis. Since biology clearly demonstrates that molecular machines are possible (living cells themselves are an example), the manufacture of bio-inspired molecular machines using biomimetic techniques is envisaged in the near future.

Nanotechnology is a multidisciplinary field with almost uncountable potential applications. A few examples are presented next. First, in the biomedical domain, nanoparticles such as dendrimers, carbon fullerenes (buckyballs) and nanoshells are currently used to target specific tissues and organs [24]. Another area where nanotechnology plays an important role is environmental science, where molecular and genomic tools are used to uncover the complexity of the induced defense signaling networks of plants [53]. Finally, in the industrial field, molecular-scale filters and pores with well-defined sizes, shapes, and surface properties allow to engineer better functionality in molecular sieving [34].

The envisaged *nanomachines* are the most basic functional units able to perform very simple tasks at the nanoscale, including computing, data storage, sensing, actuation and communication. In the electromagnetic domain, recent advances in nanotechnology have allowed the implementation of devices that perform some of these tasks, such as graphene-based nanosensors or lithium nanobatteries [6]. In the biological domain, cells are a clear example of living nanomachines. Therefore, even though a complete nanomachine has not been manufactured to date, artificial simple nanomachines are expected to become a reality in the near future. A conceptual diagram of a nanomachine in the

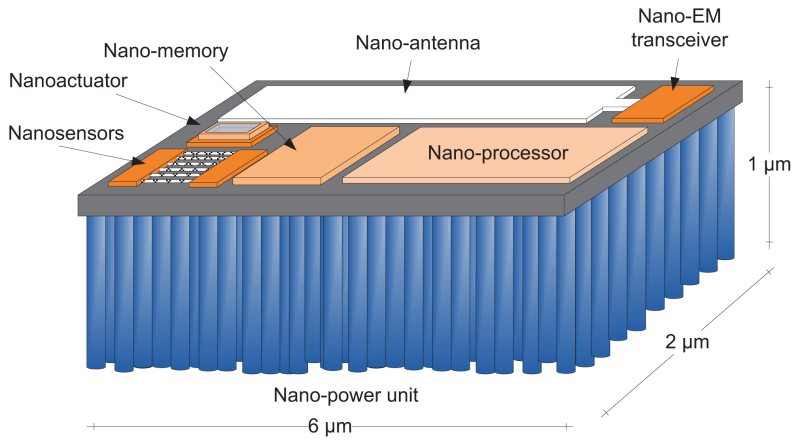

Figure 1.1: Conceptual diagram of a nanomachine in the electromagnetic domain [6].

electromagnetic domain is shown in Fig. 1.1.

1.2 Nanonetworks

Because of their tiny size, the operation range of nanomachines is limited to their close nano-environment. In consequence, a huge number of them will be required in order to perform meaningful tasks in a real scenario. These nanomachines will also need to control and coordinate their functions, leading to several research challenges in communication at the nanoscale.

Nanonetworks, the interconnection of nanomachines, provide means for cooperation and information sharing among them, allowing nanomachines to cover larger areas and fulfill more complex tasks [4]. The traditional mechanisms used in traditional communication networks, such as mechanical, acoustic and electromagnetic communication, have been found inappropriate at the nanoscale, due to the difficulty of scaling down current transceivers and energy constraints [44]. A nanonetwork is thus not a mere downscaled version of a conventional network; on the contrary, classical communication techniques need to undergo a profound revision before being applied to this new scenario. Several mechanisms have recently been proposed to interconnect nanomachines, leading to two novel network paradigms at the nanoscale: molecular communication [46] and nano-electromagnetic communication [38].

1.2.1 Molecular Communication

Molecular communication is a novel nanonetworking paradigm inspired by communication among living cells [11]. A typical cell size is of 10 µm and a typical cell mass is 1 nanogram, in the same order of magnitude than the expected size of nanomachines. This fact has led researchers to study communication mechanisms among living cells with the objective of applying them to implement nanonetworks in biological scenarios.

The molecular communication techniques found in biology are very distance-dependent. Thus, different communication techniques must be used depending on the distance between emitters and receivers. They can be classified in three categories: short-range (nm to µm), medium-range (µm to mm) and long-range (mm to m) techniques:

- For the *short range*, two methods have been proposed [4]. The first one is molecular signaling, based on encoding the information in the emission of molecules which diffuse in the medium. The second technique is based on molecular motors, protein complexes that are able to transport molecules from transmitters to receivers through microtubules. A schema of the communication process using short-range molecular communication techniques is depicted in Fig. 1.2.

- Two mechanisms have also been proposed for *medium-range* molecular communication: flagellated bacteria [30] and catalytic nanomotors [31]. Both methods are based on encoding the information in DNA sequences (a DNA packet), which are carried from transmitter to receiver using bacteria or nanomotors, respectively. Fig. 1.3 shows a diagram of these communication techniques.

- Finally, several techniques have been proposed for the *long range*, such as pheromones, pollen, spores, axons and light transduction [47], which are used by many species to communicate. An example is quorum sensing [2], a decision-making process used by bacteria to coordinate their behavior. We observe some of these methods in Fig. 1.4.

1.2.2 Nano-electromagnetic Communication

Other researchers have investigated how to communicate nanomachines by means of electromagnetic waves [6]. In this case, there are doubts about the feasibility of scaling down current metallic antennas in order to build nanoantennas, mainly because their resonant frequency is expected to be extremely high [37]. The frequency radiated by an antenna can be obtained with the expression $f = v_p/2L$, where v_p stands for the wave propagation speed inside the antenna and L is the antenna length. Thus, for the expected size of a nanomachine (a few μm^2) [6], the frequency radiated by a metallic nanoantenna would be in the optical range (hundreds of THz). Such a high frequency would result in a very large bandwidth, but also in a huge channel attenuation. This attenuation would cause the transmission range of nanomachines to be almost zero, which would render the practical implementation of nanonetworks infeasible.

In order to overcome this limitation, *graphene-based nanoantennas* [38] have been proposed to implement electromagnetic communication among nanomachines. Graphene, shown in Fig. 1.5, consists of a hexagonal lattice of carbon atoms and it is used to manufacture Carbon Nanotubes (CNT) and Graphene

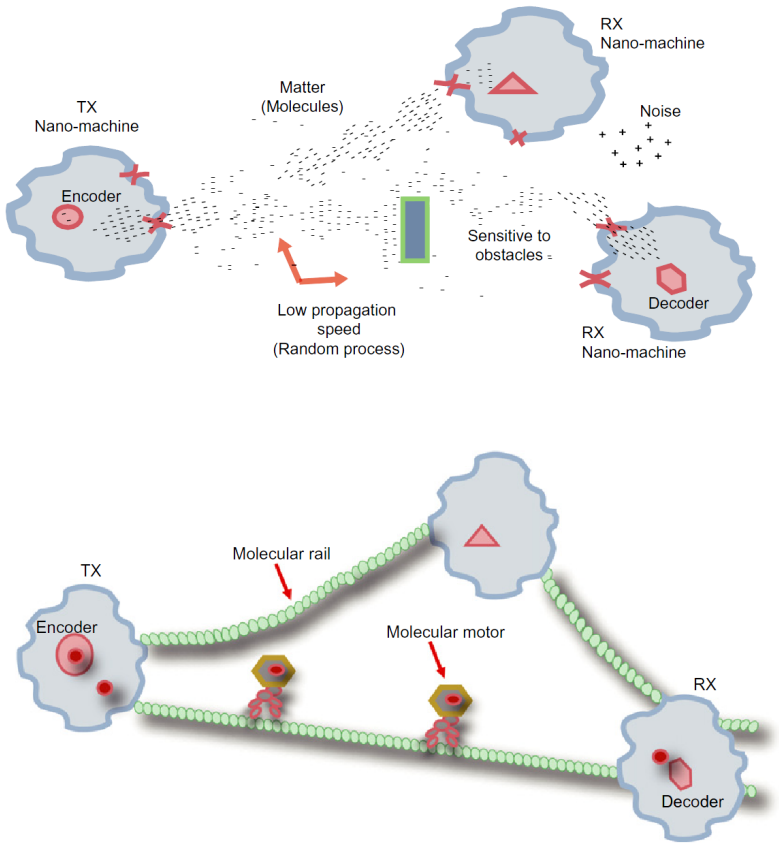

Figure 1.2: Short range molecular communication techniques: molecular signaling (top) and molecular motors (bottom) [4].

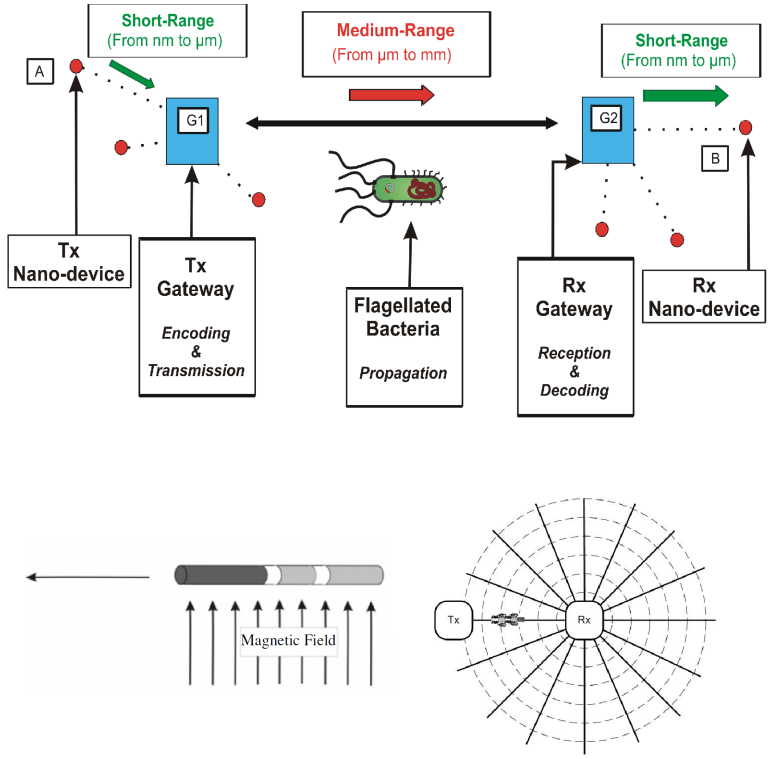

Figure 1.3: Medium range molecular communication techniques: flagellated bacteria (top) and catalytic nanomotors (bottom) [30, 31].

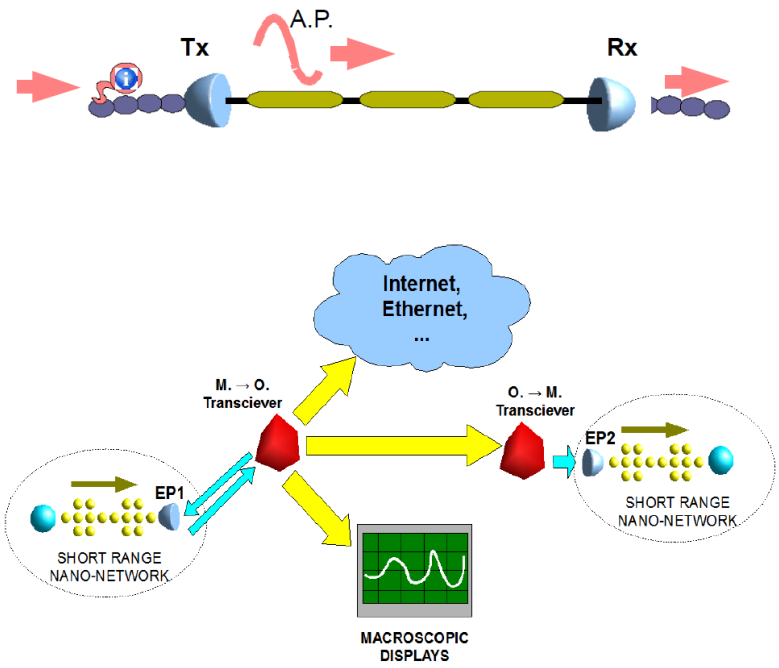

Figure 1.4: Long range molecular communication techniques: axons (top) and light transduction (bottom) [47].

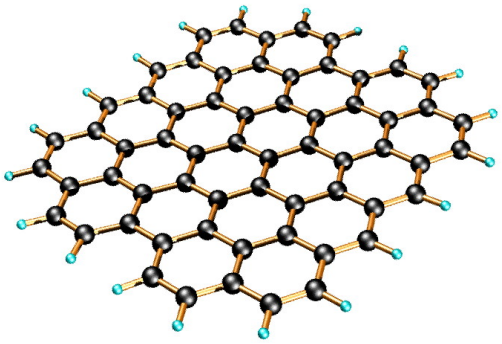

Figure 1.5: Idealized structure of a single graphene sheet.

Nanoribbons (GNR). These nanomaterials are considered to be among the main candidates to become the silicon of the 21st century [10], since they exhibit novel properties due to its regular internal structure. Due to these properties, a graphene-based nanoantenna of a size in the order of µm would resonate at a lower frequency in the terahertz band (0.1–10 THz) [38], greatly reducing the channel attenuation experienced by the radiated signals. Therefore, graphene-based nanoantennas are envisaged to allow electromagnetic communication at the nanoscale.

1.3 Applications of Nanonetworks

Nanonetworks will boost the range of applications of nanotechnology, bringing new opportunities in fields as diverse as Information and Communication Technologies (ICT) (e.g., Wireless Nanosensor Networks [6]), biomedical technology (e.g., cooperative drug delivery systems [24]) or environmental research (e.g., distributed air pollution control [34]).

A sample application from the biomedical field is an intelligent disease detection and targeted drug delivery system (Fig. 1.6, left), constituted by an intrabody distributed network of nanosensors and nanoactuators. Nanosensors that have already been successfully manufactured are able to detect lung cancer, asthma attacks, the influenza virus, or the parasite responsible for malaria [58, 64]. Several nanoactuators that have also been synthesized include nanoheaters based on magnetic nanoparticles able to kill cancer cells by heating them [21, 36], and magnetic nanoparticles and gold nanoshells which may be used as drug containers. The contained drugs are released through the application of local heat, which melts the containers [22].

Another of the main applications nanonetworks is in the field of nanosensors [54, 42]. A nanosensor is a device that makes use of the unique properties of new nanomaterials to detect and measure events at the nanoscale. Since the detection range of nanosensors is limited to their close environment, communication among nanosensors will be needed to cover larger areas. Wireless NanoSensor Networks (WNSNs) [6], a particular case of nanonetworks but

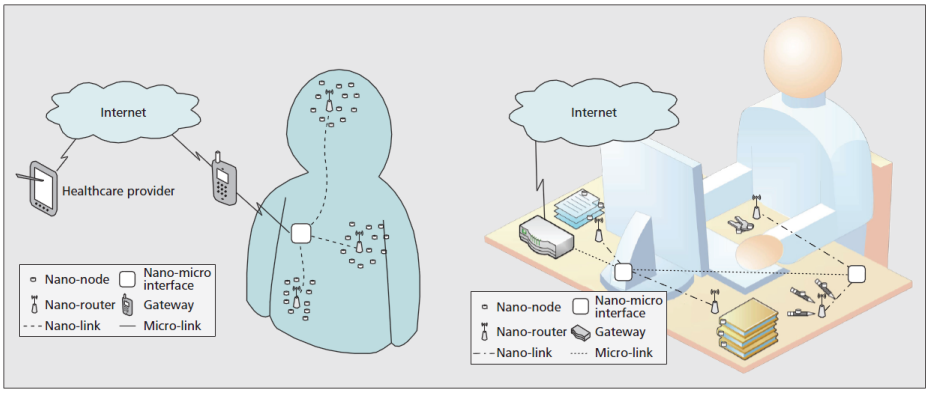

Figure 1.6: Applications of nanonetworks: intrabody nanonetworks for healthcare applications (left) and the interconnected office (right) [5].

probably one of the most promising ones, implement this communication by encapsulating nanosensors into nanomachines, which communicate in order to cooperatively monitor physical or environmental conditions over a large field. An application of WNSNs is the interconnected office [5] (Fig. 1.6, right), where every single element normally found in an office is provided of a nanotransceiver which allows it to be permanently connected to the Internet.

1.4 Motivation of this Thesis

The purpose of this thesis is to provide the means to answer a key question: do nanonetworks have the potential of becoming a *reality* or will they remain in the realm of *science fiction*? One way to obtain the answer to this question is to study the scalability of the performance metrics in a communication network, such as the throughput, the transmission delay and the energy consumption, when the network size is reduced to the nanoscale.

In this work, we lay the foundations of a scalability theory for nanonetworks, which will allow to determine the *feasibility* of nanonetworks. With this objective, we aim to analyze how the performance metrics of nanonetworks scale as the network shrinks.

It may initially seem that scalability of current electromagnetic networks, which has been thoroughly studied [3, 25, 33, 45], should also apply to nanonetworks. However, as we explained in Section 1.2, nanonetworks cannot be realized by simply reducing the size of current electromagnetic networks. On the contrary, the physical channel of both molecular and nano-electromagnetic nanonetworks presents several peculiarities. On the one hand, in the molecular communication scenario, information is encoded in molecules or DNA strings which are physically transported from the transmitter to the receiver. On the other hand, in the nano-electromagnetic case, quantum effects cause the wave propagation at the nanoscale to differ significantly from the traditional scenario. These quantum effects have their origin in the regular atomic structure of the nanomaterials used to manufacture nanomachines and in the molecular

properties of the transmission medium at the nanoscale. As a consequence, the communication metrics at the nanoscale will not necessarily be the same than their equivalent in traditional electromagnetic and optical networks.

In order to establish the scalability of the communication metrics in nanonetworks, a characterization of the nanoscale physical channel for both the molecular and the electromagnetic scenarios is first needed. In the molecular case, we concentrate in the short-range technique of molecular signaling, which has been widely studied [11, 14, 15, 43], although a characterization of the molecular channel using Fick's laws of diffussion is still missing. Moreover, to the best of our knowledge, a realistic simulation tool of diffusion-based molecular communication does not exist to date. The nano-electromagnetic physical channel, on the contrary, has been recently modeled [37], so we can use the use this model to derive the scalability of electromagnetic nanonetworks.

1.5 Main Contributions

The main outcome of this work is the study of the scalability of some of the most relevant performance metrics in nanonetworks and its comparison with the scalability of traditional electromagnetic networks. This thesis includes three main contributions leading to this objective, which are outlined next:

- First, an initial exploration of the scalability of electromagnetic nanonetworks is attempted in Chapter 2, choosing the channel capacity as communication metric. A recently-presented physical channel model for electromagnetic communication at the nanoscale is first described. Next, based on this model, an analytical framework is developed in order to evaluate how the channel capacity scales when quantum effects appear. These results are then compared with the case in which quantum phenomena are not present. In addition, asymptotic expressions for the channel capacity in the limit when the network dimensions tend to zero are formulated, and the necessary conditions to ensure the feasibility of the network at the nanoscale are established. Finally, based on these conditions, novel guidelines on the scalability of various network parameters are derived.

- Second, Chapter 3 focuses on the characterization of the physical channel of diffusion-based molecular communication. A scenario of molecular signaling, whose physical channel is governed by Fick's laws of diffusion, is considered. The molecular channel is characterized following two complementary approaches: first, the channel impulse response, transfer function and group delay are obtained; second, a pulse-based modulation scheme is proposed, and expressions for the most relevant performance evaluation metrics are analytically obtained and validated by simulation. Finally, the scalability of these metrics is compared with their equivalents in a wireless electromagnetic channel.

- Third, Chapter 4 describes *NanoSim*, a simulation framework for diffusion-based molecular communication, which has been designed in collaboration with two other master theses. The working principles of *NanoSim* are the following. Transmitters encode the information by releasing particles into the medium, thus varying their local concentration. These particles diffuse following the laws of Brownian motion. NanoSim also takes into account the collisions among them. Receivers decode the information by sensing the particle concentration in their neighborhood. The benefits of *NanoSim* include the validation of channel models for molecular communication and the evaluation of novel modulation schemes. In this work, NanoSim was used to validate the analytical results of the communication metrics obtained in Chapter 3.

We consider that the results of this work provide interesting insights as well as a useful simulation tool which may serve designers as a guide to implement future molecular and electromagnetic nanonetworks. Therefore, each of the previous contributions has led to a paper which is either submitted or in preparation.

Chapter 2

Scalability of the Channel Capacity of Electromagnetic Nanonetworks

2.1 Introduction

In this chapter, we analyze the scalability of electromagnetic communication at the nanoscale, taking as performance metric the channel capacity. Scalability theories have been paramount in the development of circuits based on CMOS technology, since they have provided a roadmap that has allowed designers to know *how* to make circuits smaller in order to optimize the desired performance metrics [17, 63, 23]. Inspired by these roadmaps, we investigate the network scalability when the size of the network shrinks to the nanoscale; this is opposite to most of the existing literature, which considers a scenario where the network size grows [33, 41, 25, 3]. Our final objective is to derive guidelines that help researchers design future nanomachines. The main contributions in this chapter are the following:

1. We find an analytical expression for the nano-electromagnetic channel capacity in the limit when the network dimensions tend to zero, as a function of three key scale parameters: nanomachine length, transmission distance and radiated power. We then compare the scalability of the capacity of graphene-based nanoantennas with respect to traditional antennas. Our results show crucial differences, demonstrating that graphene-based nanoantennas have a scalability advantage over traditional ones.

2. Based on the previous analytical framework, we particularize the capacity expressions by assuming realistic parameters. We then derive guidelines which indicate how the transmission range of nanomachines and the transmitted power need to scale as a function of the nanomachine length in order to keep the network feasible. These results provide useful insights which may serve designers as a guide to implement future nanomachines and nanonetworks.

2.2 Electromagnetic Communication at the Nanoscale

Graphene-based electromagnetic nano-transceivers and nanoantennas will operate in the terahertz band [37], a frequency range spanning the frequencies between 0.1 and 10 THz. In this section, we first review a recently-presented physical model of the nano-electromagnetic channel [37]. Next, based on this model, we identify the main differences between the nano-electromagnetic channel with respect to the traditional electromagnetic channel at the macroscale. Last, we discuss a few considerations on the bandwidth and the channel capacity of the nano-electromagnetic channel.

2.2.1 Nano-electromagnetic Physical Channel Model

Despite the major limitations of the terahertz band for medium- and long-range communications [52], results on short-range communication in the terahertz band [37] show the opportunities of this band for nanoscale communication, even for very power-constrained devices. In this section, we describe a recently-presented propagation model based on radiative transfer theory [29] that makes intensive use of the HITRAN (HIgh resolution TRANsmission molecular absorption database) line catalog [56].

Path loss

The total path loss, A, in dB for a traveling wave in the terahertz band is defined as the addition of the spreading loss, A_{spread}, and the molecular absorption loss, A_{abs}, both in dB:

$$A(f,d) = A_{spread}(f,d) + A_{abs}(f,d) \tag{2.1}$$

where f stands for the EM wave frequency and d is the path length. The *spreading loss* accounts for the attenuation due to the expansion of the wave as it propagates through the medium, and is defined in dB as:

$$A_{spread}(f,d) = 20\log\left(\frac{4\pi f d}{c}\right) \tag{2.2}$$

where c stands for the speed of light in vacuum.

The *absorption loss* accounts for the attenuation that an EM wave suffers because of molecular absorption, i.e., the process by which part of the wave energy is converted into internal kinetic energy of the excited molecules in the medium. Indeed, several molecules present in a standard medium are excited by electromagnetic radiation at certain frequencies within the terahertz band, converting part of the radiation into internal vibrations. The absorption loss A_{abs} reflects this reduction in the wave energy, and it is defined in dB as:

$$A_{abs}(f,d) = -10\log\tau(f,d) \tag{2.3}$$

where τ is the transmittance of the medium. This parameter measures the fraction of incident radiation that is able to pass through the medium and, by assuming an homogeneous medium, it can be calculated using the Beer-Lambert Law as [29]:

$$\tau\left(f,d\right)=e^{-k(f)d} \tag{2.4}$$

where k is the medium absorption coefficient, which depends on the composition of the medium, i.e., the particular mixture of molecules found along the path, and it is defined as:

$$k\left(f\right)=\sum_{i,g}k^{i,g}\left(f\right) \tag{2.5}$$

where $k^{i,g}$ is the individual absorption coefficient for the isotopologue (i.e., a molecule that only differs from another in its isotopic composition) i of gas g. For example, a standard medium is mainly composed of nitrogen (78.1%), oxygen (20.9%) and water vapor (0.1.0-10.0%), and each gas has different isotopologues that resonate at several frequencies within the terahertz band. The major contribution comes from water vapor.

The absorption coefficient of an isotopologue i of gas g, $k^{i,g}$ for a molecular volumetric density, $Q^{i,g}$ at pressure p and temperature T can be written as:

$$k^{i,g}\left(f\right)=\frac{p}{p_o}\frac{T_{STP}}{T}Q^{i,g}\sigma^{i,g}\left(f\right) \tag{2.6}$$

where p_0 and T_{STP} are the Standard-Pressure-Temperature values and $\sigma^{i,g}$ is the absorption cross section for the isotopologue i of gas g. Simply stated, the total absorption will depend on the number of molecules of a given gas that are found along the path.

Finally, we can compute the total path loss by combining equations (2.6), (2.4), (2.3), (2.2) and (2.1). In Fig. 2.1, the total path loss for an electromagnetic wave in the terahertz band is shown as a function of both frequency (x-axis) and distance (y-axis), in standard room conditions (pressure 1 atm, temperature 296 K) with 10% of water molecules. Due to the spreading loss, the total path loss increases with both distance and frequency independently of the molecular composition of the channel, similarly to conventional communication models in the megahertz or few gigahertz frequency ranges. However, the presence of several molecules along the path, and specially water vapor, defines several peaks of attenuation for distances above a few hundreds of millimeters. For shorter distances, the terahertz band can be thought of as a single transmission window almost 10 THz wide.

Noise

The ambient noise in the terahertz channel is mainly contributed by the molecular noise, generated by the absorption from molecules present in the medium. The parameter that measures this phenomenon is the emissivity of the channel, ε, and it is defined as

$$\varepsilon\left(f,d\right)=1-\tau\left(f,d\right) \tag{2.7}$$

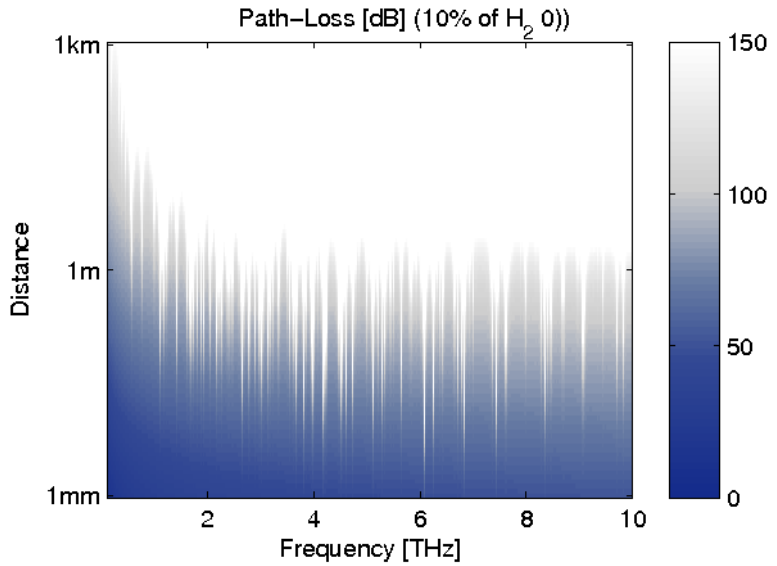

Figure 2.1: Total path loss in dB as a function of frequency f and distance d in a standard medium with 10% of water vapor molecules (the values for path loss have been truncated at 120 dB to avoid masking relevant transmission windows in the short-range).

where f is the signal frequency, d stands for the path length and τ is the transmissivity of the medium, found in Eq. (2.4).

The equivalent noise temperature due to molecular absorption T_{mol} that an omnidirectional antenna will detect from the medium is further obtained as:

$$T_{mol}(f,d) = T_0 \varepsilon(f,d) \tag{2.8}$$

where T_0 is the reference temperature. This type of noise will be only present around the resonant frequencies of the molecules in the medium. For every single resonance, the noise can be modeled as Gaussian. In addition, and more importantly, this noise will be only present when an EM wave is being radiated, i.e., there is no molecular absorption noise if nothing is exciting the molecules. This is one of the major differences with conventional Additive White Gaussian Noise, and should be further exploited in new communication schemes for nanonetworks.

To compute the equivalent noise power at the receiver, it is necessary to define the transmission bandwidth, which will in turn depend on the transmission distance and the composition of the medium. For a given bandwidth, the total noise power P_n can be calculated as:

$$P_n(f,d) = \int_B k_B T_{mol}(f,d)\, df \tag{2.9}$$

where k_B is the Boltzmann constant and B stands for the system bandwidth. In Fig. 2.2, the molecular noise temperature given by Eq. (2.8) created by an EM

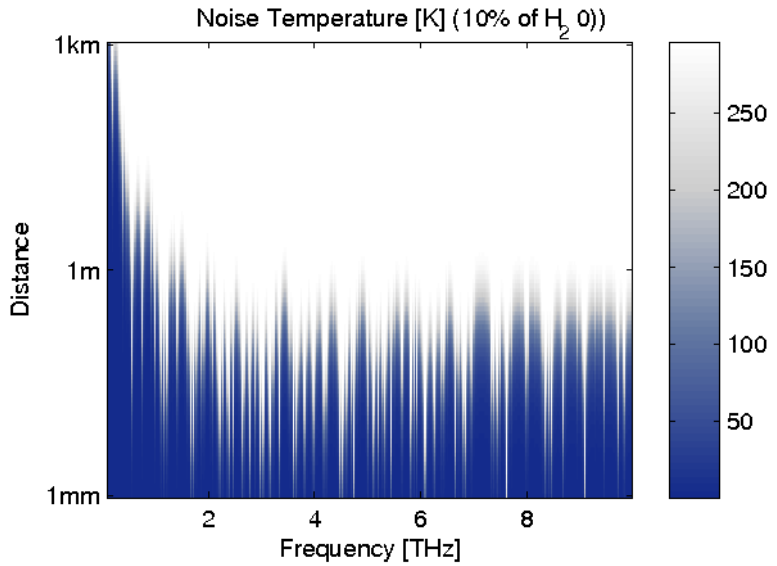

Figure 2.2: Noise temperature as a function of frequency f and distance d in a standard medium with 10% of water vapor molecules.

wave in the terahertz band is shown as a function of both frequency (x-axis) and distance (y-axis), in standard room conditions (pressure 1 atm, temperature 296 K) with 1% of water molecules. This type of noise is only significant for transmission distances above a few tens of millimeters. In addition, it has a strong frequency dependence.

More details about this physical model of the nano-electromagnetic channel may be found in a recent article [37].

2.2.2 Quantum Effects

From the study of the previously-described model, we have identified three *quantum effects* appearing at the nanoscale that will greatly impact nano-electromagnetic communication. The first one is the lower wave propagation speed which stems from using graphene-based nanoantennas, and the other two are caused by molecular absorption, a novel property of the electromagnetic channel at the terahertz band. We briefly describe these phenomena next.

Wave Propagation Speed

In a traditional metallic antenna, the wave propagation speed in vacuum is approximately equal to the speed of light c. In a graphene-based nanoantenna, however, electrons behave differently due to the regular internal structure of the carbon lattice in graphene. For example, transport of electrons within graphene suffers virtually no scattering, which results in an effect known as bal-

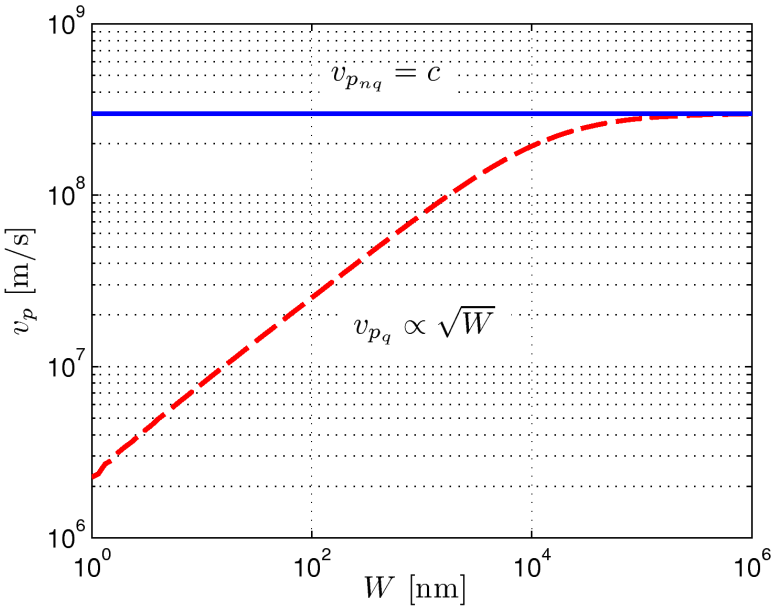

Figure 2.3: Log-log plot of the wave propagation speed as a function of the antenna width W, without quantum effects ($v_{p_{nq}}$, blue solid line) and with quantum effects (v_{p_q}, red dashed line).

listic transport [26]. Moreover, the wave propagation speed inside a graphene-based nanoantenna can reach a value, depending on the antenna size, up to 100 times smaller than the speed of light [35, 13]. Furthermore, when these quantum effects are present, the wave propagation speed has been observed to scale with the antenna width [38]. Using curve fitting, we have found this scalability to be proportional to the square root of the antenna width, for an antenna width of up to 10 µm and an antenna length much larger than its width. Fig. 2.3 shows a comparison between the wave propagation speed with and without accounting for the quantum effects.

A consequence of the lower wave propagation speed in a graphene-based nanoantenna is that the resonant frequency of the propagated wave may be up to two orders of magnitude below the frequency obtained with an antenna of the same size built with non-carbon materials. Thinking of a device with a nanoantenna just a few µm long (e.g., a nanosensor device), building the antenna with graphene yields a resonant frequency in the teraherthz band (0.1–10 THz) [38], whereas a traditional antenna would resonate in the optical range.

Molecular Absorption

Molecular absorption is the process by which part of the wave energy is converted into internal kinetic energy of the excited molecules in the medium. As described in Section 2.2.1, molecular absorption acts as an additional factor of attenuation to the propagated signal in nano-electromagnetic communication.

In addition, the absorption from molecules present in the medium does not only attenuate the transmitted signal, but it also introduces noise. Thus, molecular noise needs to be taken into account as a new source of noise in nano-electromagnetic communication.

2.2.3 Bandwidth and Channel Capacity

Since the electromagnetic waves radiated by a graphene-based nanoantenna have a frequency in the terahertz band, the corresponding bandwidth associated to this frequency and, ultimately, the capacity of the nano-electromagnetic channel is expected to be very high. One may think that such a large capacity will not be needed, since a single nanomachine will not need to transmit a huge amount of data. However, we think that a large channel capacity will be of great benefit to nanonetworks.

In current communication networks, the channel capacity is usually the bottleneck that limits the throughput of the network. In consequence, network protocols are designed with the aim of minimizing bandwidth consumption in order to optimize the network performance. The envisaged huge channel capacity of nanonetworks opens the door to novel protocols that take advantage of a virtually unlimited bandwidth to optimize other crucial performance metrics, such as the nanomachine complexity or its energy consumption.

2.3 Nano-electromagnetic Channel Capacity

The goal of this section is to find an analytical expression for the nano-electromagnetic channel capacity in the limit when the network dimensions tend to zero, as a function of three key scale parameters: (i) the nanomachine length Δ, (ii) the transmission distance d, and (iii) the total power radiated by the transmitter P_T. We perform this analysis for two scenarios: (i) when the quantum effects introduced in the previous section are not present (i.e., the transmitters use traditional antennas to radiate the electromagnetic signal), and (ii) when these quantum phenomena appear (i.e., graphene-based nanoantennas are used). The first scenario is taken as a reference in order to evaluate the results obtained in the latter case. Table 2.1 shows the parameters and constants used throughout this section.

As we outlined in the previous section, a graphene-based nanoantenna is able to radiate EM waves in the terahertz band. In consequence, the nano-electromagnetic channel is expected to have a very large bandwidth [37] and in consequence a highly frequency-selective behavior. Thus, in order to compute its capacity, we need to divide the channel in narrow sub-bands so that, in each sub-band, the channel attenuation and the noise power spectral density can be considered locally flat. The total channel capacity will then be the combined capacity of all its sub-bands. We obtain the capacity of a single sub-band C_i

Symbol	Quantity
Δ	Nanomachine length
d	Transmission distance
P_T	Total power radiated by the transmitter
f	Antenna resonant frequency
B	Total system bandwidth
v_p	Propagation speed of the wave inside the antenna
L	Antenna length
c	Speed of light in the vacuum
$S(f)$	Power spectral density of the radiated signal at the transmitter
$A(f)$	Total channel attenuation
A_{spread}	Spreading loss
A_{abs}	Molecular absorption loss
τ	Transmittance of the medium
k	Medium absorption coefficient
$N(f)$	Power spectral density of noise at the receiver
k_B	Boltzmann constant
T_{sys}	System temperature
T_{mol}	Molecular noise temperature
T_0	Standard temperature
ε	Emissivity of the medium

Table 2.1: Parameters and constants.

using the Shannon limit theorem [57]:

$$C_i = B_i \log_2 \left(1 + \frac{S_i}{A_i N_i}\right) \tag{2.10}$$

where B_i is the width of the frequency band, S_i the power radiated by the transmitter in this band, A_i the sub-band attenuation and N_i the noise power in the frequency band.

The total channel capacity C can be obtained by taking the limit of the sub-band capacity when $B_i \to 0$ and integrating it over the whole frequency band, which leads to the following expression [28]:

$$C = \max_{S(f):\int_B S(f)df \leq P_T} \int_B \log_2 \left(1 + \frac{S(f)}{A(f)N(f)}\right) df \tag{2.11}$$

where $S(f)$ is the radiated power spectral density, $A(f)$ stands for the channel attenuation and $N(f)$ is the noise power spectral density at the receiver.

In order to find an expression for the channel capacity C as a function of the scale parameters, we first concentrate on the magnitudes that determine the channel capacity, which appear in Eq. (2.11): the channel bandwidth B, the radiated power spectral density $S(f)$, the channel attenuation $A(f)$ and the noise power spectral density $N(f)$. Next, we express each of them as a

function of the scale parameters Δ, d and P_T, for the two previously-mentioned scenarios: with and without quantum effects. Finally, we combine these results in order to find an analytical expression of the nano-electromagnetic channel capacity.

2.3.1 Channel Bandwidth

As shown in Section 2.2.1, if the transmission distance d is sufficiently small, the available bandwidth is the whole terahertz band, from zero to the highest frequency radiated by the antenna. Thus, in order to find an expression for the channel bandwidth as a function of the scale parameters, we first need to compute the radiated frequency f. The first resonant frequency of a nanoantenna (or any other type of resonator) is given by the expression:

$$f = \frac{v_p}{2L} \tag{2.12}$$

where v_p denotes the wave propagation speed inside the antenna and L is the antenna length. The wave propagation speed inside an antenna depends on its type. As stated in Section 2.2.2, if the antenna is metallic, quantum effects do not appear and the wave propagation speed is $v_{p_{nq}} = c$. However, if the antenna is made of graphene, the quantum phenomena cause the wave propagation speed to scale with the square root of the antenna width (which we assume proportional to its length), i.e., $v_{p_q} = k_1\sqrt{\Delta}$, where k_1 is a proportionality constant and Δ is the nanomachine length. We approximate the antenna length by the length of the whole nanomachine ($L = \Delta$). Then, we obtain an expression for the frequency of the propagated wave which varies depending on whether quantum effects are present or not:

$$f_{nq} = \frac{c}{2\Delta} \tag{2.13}$$

$$f_q = \frac{k_1}{2\sqrt{\Delta}} \tag{2.14}$$

Throughout this chapter, we use the subindex nq to denote the parameters corresponding to the traditional case (no quantum effects), and the subindex q for the case when quantum phenomena are considered.

Since we assume that the system bandwidth for a nanoantenna is equal to its operating frequency ($B = f$), its expression as a function of the scale parameters is the same:

$$B_{nq} = \frac{c}{2\Delta} \tag{2.15}$$

$$B_q = \frac{k}{2\sqrt{\Delta}} \tag{2.16}$$

2.3.2 Transmitted Power Spectral Density

Modulations based on the transmission of very short Gaussian pulses have recently been proposed for nano-electromagnetic communication [6]. A pulse-based scheme is a promising candidate to modulate the electromagnetic waves radiated by a nanomachine because of the simplicity to generate and detect pulses (since there is no carrier) and its high spectral efficiency (a very short Gaussian pulse virtually occupies the whole frequency band). In consequence, the power spectral density of these pulses is approximately flat over the whole frequency band. Therefore, we approximate it by a uniform power spectral density:

$$S(f) = \begin{cases} P_T/B & \text{if } 0 < f < B, \\ 0 & \text{otherwise.} \end{cases} \tag{2.17}$$

where P_T is the total power radiated by the transmitter.

2.3.3 Channel Attenuation

As we introduced in Section 2.2.1, the attenuation of the nano-electromagnetic channel has two main components: the spreading loss A_{spread} and the molecular absorption loss A_{abs}. As presented in Section 2.2.1, molecular absorption loss can be expressed as:

$$A_{abs} = \frac{1}{\tau} = e^{kd} \tag{2.18}$$

where τ is defined as the transmittance of the medium, and k is the medium absorption coefficient. Since we are interested in the scenario where the transmission distance d tends to zero, we observe that in the limit $d \to 0$ the value of the molecular absorption loss tends to 1:

$$\lim_{d \to 0} A_{abs} = \lim_{d \to 0} e^{kd} = 1. \tag{2.19}$$

Therefore, we conclude that molecular absorption loss will have a negligible effect on nano-electromagnetic communication. The total attenuation can thus be approximated by the spreading loss, given in the far field by the well-known expression for the free-space path loss:

$$A(f) = A_{spread} = \left(\frac{4\pi f d}{c} \right)^2. \tag{2.20}$$

2.3.4 Noise Power Spectral Density

Finally, there are two main contributors to the receiver noise at the nanoscale: thermal noise and molecular noise [37]. The total noise power spectral density in the receiver $N(f)$ can be calculated as the Boltzmann constant k_B multiplied by the total noise temperature:

$$N(f) = k_B(T_{sys} + T_{mol}) \tag{2.21}$$

where T_{sys} the system temperature and T_{mol} the molecular noise temperature. As presented in Section 2.2.1, the molecular noise temperature can be expressed as follows:

$$T_{mol} = T_0\varepsilon = T_0(1-\tau) = T_0(1-e^{-kd}) \tag{2.22}$$

where T_0 is the standard temperature, ε is known as the emissivity of the medium, τ is the transmittance of the medium and k the medium absorption coefficient. As it happened with molecular absorption, molecular noise tends to disappear when the transmission distance is small:

$$\lim_{d\to 0} T_{mol} = \lim_{d\to 0} T_0(1-e^{-kd}) = 0. \tag{2.23}$$

In consequence, the main contributor to the noise power spectral density at the nanoscale is the thermal noise. Approximating the system temperature by the standard temperature $T_0 = 293K$, we obtain a constant noise power spectral density in the whole frequency band, which we denote by N_0:

$$N(f) = k_B T_{sys} = k_B T_0 = N_0 \tag{2.24}$$

2.3.5 Expression of the Channel Capacity

Now, by combining the expressions obtained in (2.17), (2.20) and (2.24) with the definition of the channel capacity (2.11), we obtain the capacity of a nano-electromagnetic communication channel:

$$\begin{aligned} C &= \int_0^B \log_2\left(1+\frac{P_T/B}{\left(\frac{4\pi f d}{c}\right)^2 N_0}\right) df \\ &= \frac{B}{\log 2}\log\left(1+\frac{P_T c^2}{(4\pi d)^2 B^3 N_0}\right) \\ &\quad + \frac{\sqrt{P_T}c}{2\log(2)\pi d\sqrt{N_0 B}}\arctan\frac{4\pi d B^{3/2}\sqrt{N_0}}{\sqrt{P_T}c} \end{aligned} \tag{2.25}$$

Recalling the expressions for the channel bandwidth found in Section 2.3.1, we can express the channel capacity C as a function of the nanomachine size Δ, the transmission distance d and the radiated power P_T (c, N_0 and k_1 are constants):

$$\begin{aligned} C_{nq} &= \frac{c}{2\log(2)\Delta}\log\left(1+\frac{\Delta^3 P_T/d^2}{2\pi^2 c N_0}\right) \\ &\quad + \frac{\sqrt{c\Delta P_T/d^2}}{\log(2)\pi\sqrt{2N_0}}\arctan\frac{\pi\sqrt{2cN_0}}{\sqrt{\Delta^3 P_T/d^2}} \end{aligned} \tag{2.26}$$

$$\begin{aligned} C_q &= \frac{k_1}{2\log(2)\sqrt{\Delta}}\log\left(1+\frac{c^2\Delta^{3/2}P_T/d^2}{2\pi^2 N_0 k_1^3}\right) \\ &\quad + \frac{c\sqrt[4]{\Delta}\sqrt{P_T/d^2}}{\log(2)\pi\sqrt{2N_0 k_1}}\arctan\frac{\pi\sqrt{2N_0 k_1^3}}{\sqrt{P_T/d^2}c\Delta^{3/4}} \end{aligned} \tag{2.27}$$

where we have isolated the factor P_T/d^2 in both expressions. We will see the capital importance of this quotient on the scalability of the nano-electromagnetic channel capacity in Section 2.4.

2.3.6 Quantitative Results

In order to obtain quantitative results of the channel capacity as a function of Δ and d, we take equations (2.26) and (2.27) and assign values to their parameters. With this purpose, we choose realistic numbers for an envisaged scenario of nanonetworks. Next, we describe these values and the rationale behind the choices made.

When quantum effects are not present (i.e., for a metallic nanoantenna), the value of the wave propagation speed is equal to the speed of light: $v_{p_{nq}} = c$. By contrast, if the nanoantenna is built with graphene, because of quantum phenomena the wave propagation speed has been empirically observed to depend on the nanoantenna size as $v_{p_q} \approx 10^8\sqrt{\Delta}$ m/s, where Δ is the nanomachine length [38].

We assume a modulation based on femtosecond-long Gaussian pulses, which has been proposed as one of the main candidates to implement electromagnetic communication at the nanoscale [6]. We take as average transmitted power P_T of this modulation a value of 1 kW, which corresponds to a pulse having an energy of 100 pJ and a duration of 0.1 ps [37].

Concerning molecular absorption and noise, the medium absorption coefficient of a standard atmosphere has been found to have a maximum value of approximately $k_{max} = 3.5$ m^{-1} [37]. Then, considering typical transmission distances for nanomachines of up to $d_{max} = 1$ cm, the maximum value of molecular absorption in a realistic scenario of a nanonetwork is $A_{abs} = e^{k_{max}d_{max}} \approx 1.036$, which is negligible in comparison with the attenuation due to the much larger spreading loss. This result confirms that molecular absorption will not have a significant effect on communication in short-range nanonetworks, as we had previously obtained analytically. Similarly, the contribution of molecular noise is also negligible in comparison with thermal noise: $T_{mol} = T_0(1 - e^{-k_{max}d_{max}}) \approx 0.034T_0$. Regarding thermal noise, its spectral density has a value of $N_0 = k_B T_0 \approx 1.38 \cdot 10^{-23} \cdot 293$ W/Hz.

Finally, we select a realistic range of values for the nanomachine length Δ and the transmission distance d. For the former, we choose the interval between 0.1 and 10 µm, and from 1 to 10 mm for the latter. In both cases, the chosen values are inspired by the range of envisaged values for nanosensors [6]. A summary of the chosen parameters is shown in Table 2.2. Fig. 2.4 presents the quantitative results of the channel capacity when quantum effects are not present, and Fig. 2.5 when they affect the communication.

The results obtained when evaluating equations (2.26) and (2.27) show that the behavior of the nano-electromagnetic channel capacity differs significantly depending on whether we consider or not in our analysis the quantum phenomena which stem from the use of graphene-based nanoantennas. We observe that, on the one hand, the absolute value of the channel capacity is

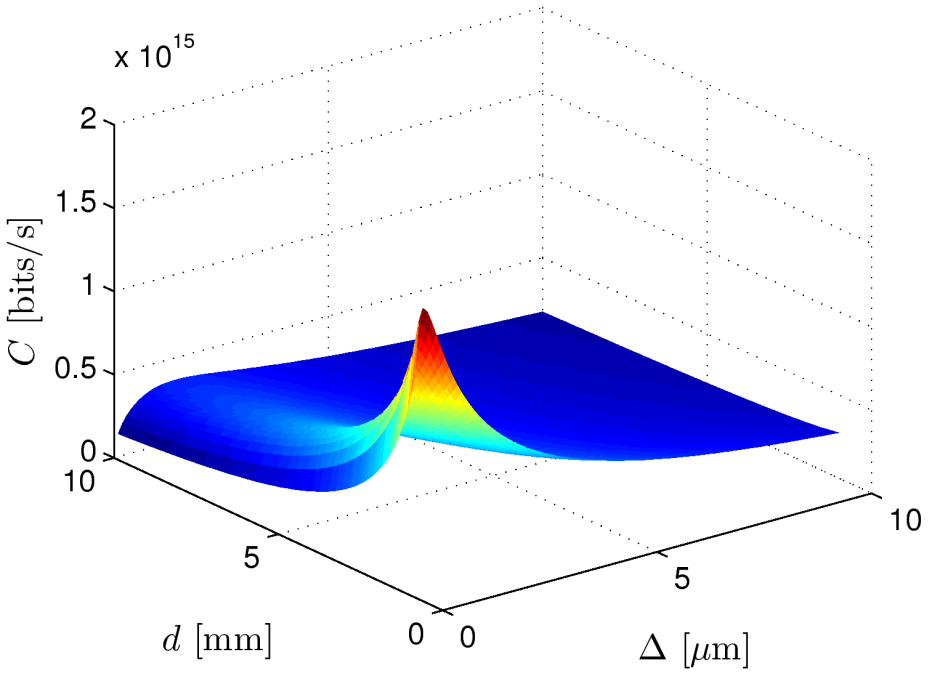

Figure 2.4: Quantitative values of the channel capacity C as a function of the nanomachine size Δ and the transmission distance d, without quantum effects.

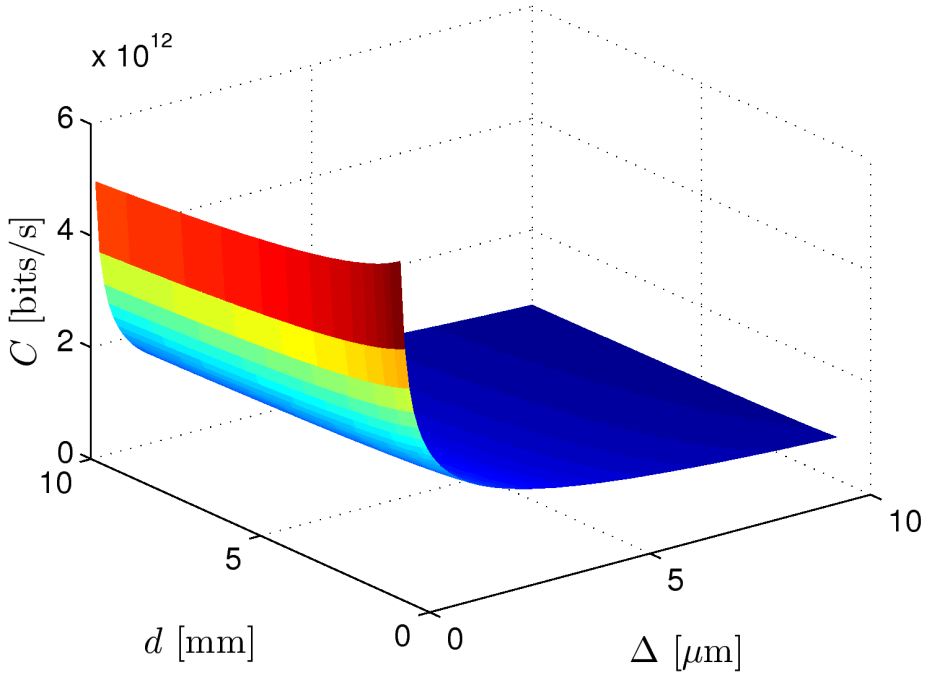

Figure 2.5: Quantitative values of the channel capacity C as a function of the nanomachine size Δ and the transmission distance d, with quantum effects.

Symbol	Quantity	Value
Δ	Nanomachine length	0.1–10 µm
d	Transmission distance	1–10 mm
P_T	Total power radiated by the transmitter	1 kW
$v_{p_{nq}}$	Propagation speed of the wave inside the antenna, without quantum effects	$3 \cdot 10^8$ m/s
v_{p_q}	Propagation speed of the wave inside the antenna, with quantum effects	$10^8\sqrt{\Delta}$ m/s
k_B	Boltzmann constant	$1.38 \cdot 10^{-23}$ J/K
T_0	Standard temperature	293 K

Table 2.2: Values chosen for the parameters.

higher when quantum effects are not present. On the other hand, while without quantum effects there is a peak in the channel capacity for a value of Δ of a few µm, when quantum effects are present the channel capacity increases monotonically as Δ decreases. This observation suggests that the scalability of the channel capacity when the network shrinks may be better than what one would expect thanks to the aforementioned quantum phenomena.

Furthermore, note that these results assume that the transmitted power is constant, which might not be realistic in some scenarios. For this reason, we next take an analytical approach and compute the limits of the channel capacity when Δ, d and P_T all tend to zero.

2.4 Limits of the Channel Capacity

We are interested in finding closed formulas for the channel capacity expressions given by the equations (2.26) and (2.27) in the limit when $\Delta \to 0$, $d \to 0$ and $P_T \to 0$. Unfortunately, these limits are not unique, but they depend on the relationships among Δ, d and P_T. Thus, in order to find an analytical expression for the capacity of a nano-electromagnetic channel, we need to assume a given relationship among the scale parameters. Following an approach as general as possible, we express d and P_T as a function of Δ as follows:

$$d = k_2 \Delta^{\alpha} \tag{2.28}$$

$$P_T = k_3 \Delta^{\beta} \tag{2.29}$$

where k_2 and k_3 are constants and α and β are real positive exponents. In other words, when the nanomachine size Δ decreases, both the transmission distance d and the transmitted power P_T shrink as well, at relative rates α and β, respectively. Under these assumptions, we can express the channel capacity as a function of a single scale parameter Δ, obtaining the following expressions:

$$\begin{aligned} C_{nq} = \frac{k_{11}}{\Delta} \log\left(1 + k_{12}\Delta^{\beta-2\alpha+3}\right) \\ + k_{13}\Delta^{\frac{\beta-2\alpha+1}{2}} \arctan\left(k_{14}\Delta^{\frac{2\alpha-\beta-3}{2}}\right) \end{aligned} \tag{2.30}$$

$$C_q = \frac{k_{21}}{\sqrt{\Delta}} \log\left(1 + k_{22}\Delta^{\beta-2\alpha+\frac{3}{2}}\right) + k_{23}\Delta^{\frac{\beta-2\alpha+1/2}{2}} \arctan\left(k_{24}\Delta^{\frac{2\alpha-\beta-3/2}{2}}\right) \tag{2.31}$$

where k_{ij}, $i \in [1,2]$, $j \in [1,4]$ are constants w.r.t. Δ. The limits when $\Delta \to 0$ of the previous expressions are functions of the parameters α and β:

$$\lim_{\Delta\to 0} C_{nq} = \begin{cases} \infty & \text{if } \beta - 2\alpha > -1, \\ \text{constant} & \text{if } \beta - 2\alpha = -1, \\ 0 & \text{if } \beta - 2\alpha < -1. \end{cases} \tag{2.32}$$

$$\lim_{\Delta\to 0} C_q = \begin{cases} \infty & \text{if } \beta - 2\alpha > -1/2, \\ \text{constant} & \text{if } \beta - 2\alpha = -1/2, \\ 0 & \text{if } \beta - 2\alpha < -1/2. \end{cases} \tag{2.33}$$

The term $\beta - 2\alpha$ in the expressions above stems from the quotient $P_T/d^2 = \Theta\left(\Delta^{\beta-2\alpha}\right)$ that appears repeatedly in the capacity expressions (2.26) and (2.27).

We define the *feasible region* of the network as the scenario where the channel capacity does not tend to zero when the network shrinks, i.e., the conditions under which $C = \Omega(1)$ when $\Delta \to 0$. As shown in Fig. 2.6, we identify three clearly differentiated regions as a function of α and β:

- The region $-1/2 \leq \beta - 2\alpha$ is feasible both when quantum effects are present and when they are not.
- The region $-1 \leq \beta - 2\alpha < -1/2$ is feasible only when quantum effects are present.
- The region $\beta - 2\alpha < -1$ is never feasible.

We thus conclude that: (i) the scalability of the relationship P_T/d^2 will be a key parameter of electromagnetic nanonetworks, since it will determine the feasibility of the network, (ii) the quantum effects derived from the use of graphene-based nanoantennas yield a larger feasible region as compared to using traditional antennas, and (iii) this scalability advantage stemming from the aforementioned quantum effects allows a reduction of the quotient P_T/d^2 up to a factor of $\Theta\left(\Delta^{1/2}\right)$ when the network shrinks.

2.5 Scalability guidelines

Enormous challenges need to be faced by the scientific community when designing electromagnetic nanonetworks. First, as it happens in current wireless networks, power consumption is envisaged to become a bottleneck in the performance of nanonetworks. Hence, one of these challenges is the fabrication of nanoscale power sources able to provide energy to nanomachines. Fortunately,

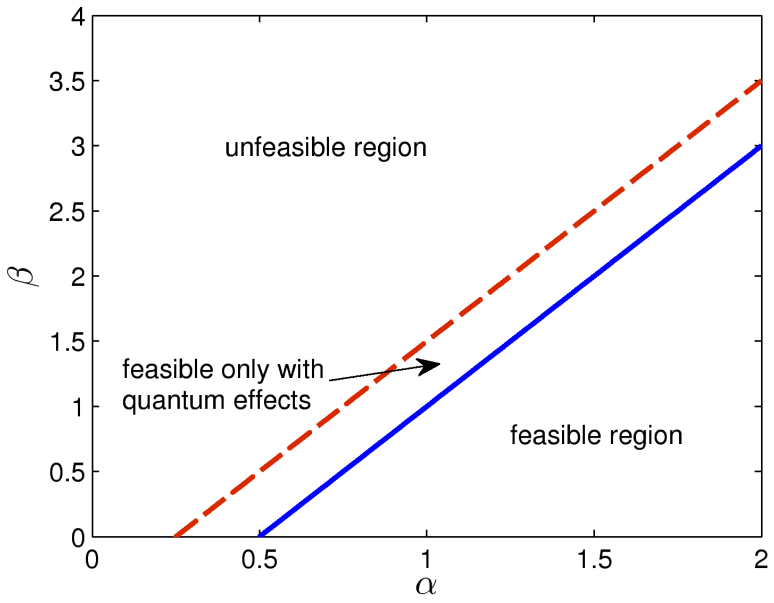

Figure 2.6: Feasible area of the channel capacity as a function of α and β. The blue solid line corresponds to the case when quantum effects are not present, and the red dashed line when they are.

researchers are actively working on novel nanomaterials and techniques to create nanobatteries [60], as well as nanoscale energy-harvesting modules [62].

Besides the power source, another important challenge of nanonetworks is the expectedly large density of nanomachines required to cover a certain region. Indeed, because of the very limited transmission range of nanomachines, and since the number of devices N needed to cover a fixed 3-dimensional area scales with their transmission range as $N = \Theta\left(d^{-3}\right)$, it seems likely that a huge number of devices will be required to build a nanonetwork. The cost of manufacturing such a number of nanomachines may therefore compromise the feasibility of the nanonetwork.

With the latter concern in mind, we establish an additional condition for the network feasibility. Besides the constraint introduced in the previous section that the channel capacity does not tend to zero when the network shrinks, we restrict the total number of nanomachines N to be inversely proportional to the volume of a single device V, i.e., $N \propto 1/V$. The rationale behind this choice is that, in this scenario, the combined volume of all the nanomachines NV (and thus their cost) will be constant. Since the volume of a nanomachine scales as $V = \Theta\left(\Delta^3\right)$, this condition results in $\Theta\left(d^{-3}\right) = \Theta\left(\Delta^{-3}\right)$. From this expression, we derive that the additional necessary condition is $d = \Theta(\Delta)$. In other words, all the network dimensions (nanomachine size and transmission distance) must shrink proportionally so as to guarantee the network feasibility.

In this scenario, which corresponds to $\alpha = 1$, recalling the results obtained in Section 2.4, we find that the feasible region of the network corresponds to the values $\beta \leq 1$ when quantum effects are not present, and $\beta \leq 3/2$ when

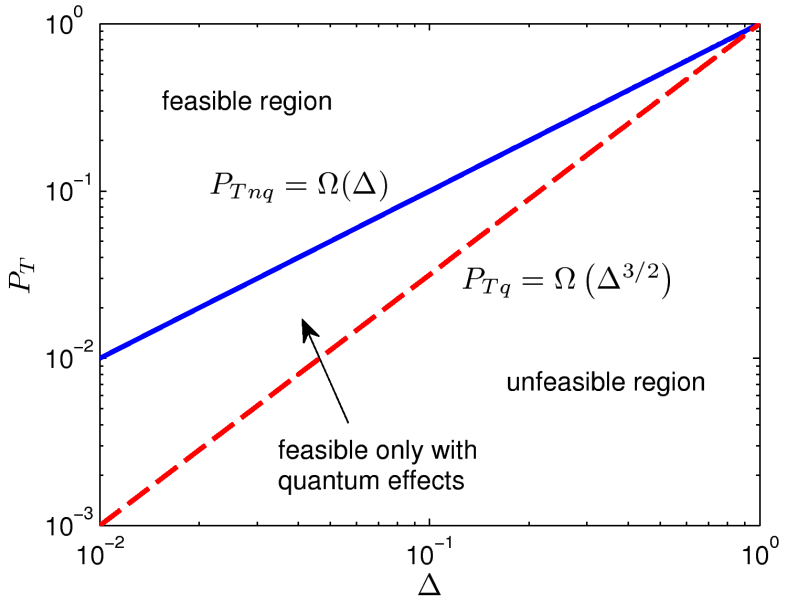

Figure 2.7: Log-log plot comparing the scalability of the transmitted power without quantum effects ($P_{T_{nq}}$, blue solid line) and with quantum effects (P_{T_q}, red dashed line), as a function of the nanomachine size Δ. The transmission distance scales as $d = \Theta(\Delta)$.

they appear. In other words, without quantum effects, the transmitted power needs to scale at most linearly with the nanomachine size, as $P_{T_{nq}} = \Omega(\Delta)$; a faster scaling would render the network infeasible. By contrast, quantum phenomena allow a faster decrease in the transmitted power, at a rate of $P_{T_q} = \Omega\left(\Delta^{3/2}\right)$. Both cases are compared in Fig. 2.7. In consequence, quantum effects achieve a scaling advantage of $\Theta\left(\Delta^{1/2}\right)$ with respect to the traditional scenario. We extract the following scalability guideline: the use of graphene-based nanoantennas allows relaxing the requirements for nanobatteries and nano-energy harvesting modules that will power nanomachines. For instance, when the size of a nanomachine is reduced by two orders of magnitude, the required energy is *one order of magnitude smaller* when using graphene-based nanoantennas with respect to the traditional case.

Chapter 3

Diffusion-based Channel Characterization in Molecular Nanonetworks

3.1 Introduction

Several techniques have been proposed to interconnect nanomachines by drawing inspiration from biology [4, 43]. Among them is calcium signaling [14], a particular case of molecular signaling. Calcium signaling is one of the most common techniques for intra- and inter-cellular communication, based on the use of calcium ions (Ca^{2+}) to encode and transmit information. As other researchers have done [46, 61], we propose calcium signaling as a method to realize communication among nanomachines in the short range (nm to µm).

The propagation of a low concentration of calcium ions in a fluid environment is a particular case of molecular diffusion. Several researchers have attempted to model the diffusion-based molecular channel; some of them have focused on its channel transfer function [50], while others have determined the channel capacity from an information-theoretical point of view [9, 51, 8]. However, to the best of our knowledge, none of them provides a system characterization for a scenario dominated by Fick's laws of diffusion [48], which we consider a realistic model for molecular signaling.

In this work, we focus on a diffusion-based molecular communication whose physical channel is governed by Fick's laws of diffusion. First, we obtain the impulse response, the transfer function and the group delay of the molecular channel. Further, we propose a pulse-based modulation scheme which we use to derive analytical expressions of relevant communication metrics, namely, the pulse delay, amplitude and width. These results are validated using *NanoSim*, a simulation framework for diffusion-based molecular communication which is thoroughly described in Chapter 4. Furthermore, the scalability of these metrics is compared with their equivalents in a wireless electromagnetic channel. Finally, the highest achievable bandwidth is analyzed and a scenario with multiple simultaneous transmitters is evaluated.

3.2 Diffusion-based Molecular Channel and Modulation Scheme

The *molecular channel* that we aim to characterize can be described as a set of nanomachines which communicate through molecular diffusion in a fluid medium. Transmitter nanomachines encode the information to be sent into a molecular release pattern. The emitted molecules cause a variation in their local concentration, which propagates throughout the medium. Receivers are able to estimate the concentration of molecules in their neighborhood and, from this measurement, recover the release pattern and decode the sent information.

In our envisaged scenario, the concentration of emitted molecules is much lower than the concentration of the fluid molecules. Under these conditions, we assume that interaction among the emitted molecules (e.g., collisions and electrostatic forces) can be neglected. An example of this kind of scenario is calcium signaling among cells, where extracellular concentration of calcium ions is in the millimolar range [15], while the concentration of water (the main component of extracellular fluid) is of 55.5 molar, more than 4 orders of magnitude higher.

In this scenario, each of the molecules released by a transmitter moves according to Brownian motion. Since the movement of each molecule is independent, molecular diffusion can be modeled by Fick's laws of diffusion with a homogeneous diffusion coefficient both in space and time. In this case, the diffusion equations are linear [59].

We propose a pulse-based modulation scheme for diffusion-based molecular communication. According to this scheme, whenever a transmitter nanomachine wants to communicate some information to its neighbors (e.g., after it detects an infectious virus [64]), it instantaneously releases a pulse of molecules. This creates a spike in the molecular concentration at the transmitter location, which then propagates through space and time. The propagation of this pulse can be analytically modeled by solving Fick's laws of diffusion. If the transmitter releases Q molecules at the instant $t = 0$, the molecular concentration at any point in space is given by [12]:

$$c(r,t) = \frac{Q}{(4\pi Dt)^{3/2}} e^{-r^2/4Dt} \tag{3.1}$$

where D is the diffusion coefficient of the medium, t is time and r is the distance from the transmitter location.

It should be noted that, since the emitted molecules do not interact among them, the previous scheme allows for simultaneous transmissions by multiple nanomachines. Interferences may be avoided if transmitters use different molecule types, in a mechanism known as Molecular Division Multiple Access (MDMA) [47].

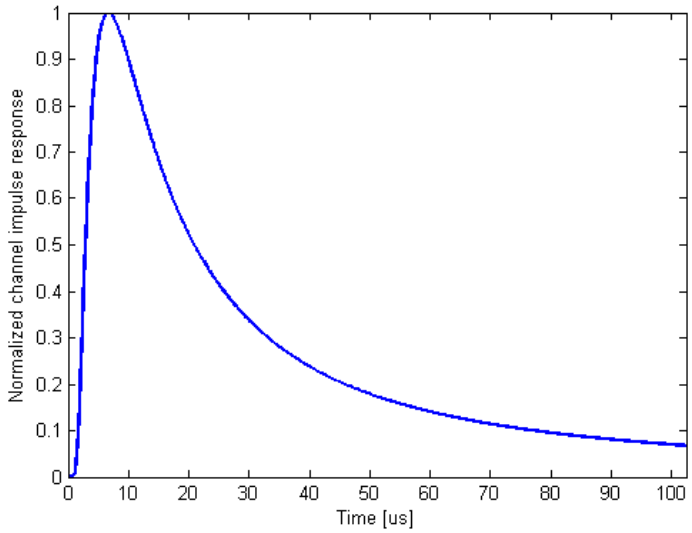

Figure 3.1: Normalized channel impulse response.

3.3 Molecular Channel Analysis

Eq. (3.1) allows to obtain the concentration measured by a receiver located at a distance r from the transmitter as a function of time. Since the previously described molecular channel is linear and time-invariant, this measure can be interpreted as the channel response to an impulse of molecules, i.e., the channel impulse response.

Fig. 3.1 shows the impulse response of the molecular channel, normalized to values between 0 and 1. We set the transmission distance to $r = 200$ nm and the diffusion coefficient to $D = 1$ nm^2/ns, similar to the diffusion coefficient of ionic calcium in cytoplasm [18]. We can observe that the concentration initially measured by the receiver is zero, but it sharply increases until reaching its maximum. The time instant at which this maximum occurs can be interpreted as the pulse delay. After the concentration peak is reached, the impulse response slowly decreases, forming a long tail due to the effect of diffusion.

We then obtain the channel transfer function by computing the Fourier transform of the impulse response. The magnitude of the channel transfer function, shown in Fig. 3.2 in dB, can be interpreted as the channel attenuation. The results indicate that only low-frequency signals can be reliably transmitted through the channel. We observe a notch at $f = 500$ kHz, related to the delay caused by the diffusion process.

Fig. 3.3 shows the molecular channel group delay. At low frequencies, we observe two peaks: a positive peak at $f = 0$ Hz and a negative one at $f = 500$ kHz. The latter one is due to the delay that causes the notch in the channel transfer function at the same frequency. At higher frequencies, the channel group delay is approximately zero.

In Fig. 3.4 and Fig. 3.5, we plot the magnitude of the normalized channel transfer function and the group delay, respectively, as a function of both the

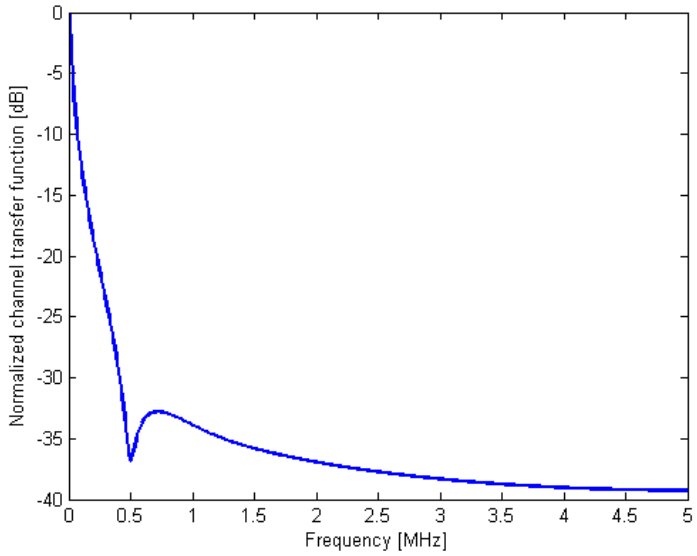

Figure 3.2: Magnitude of the normalized channel transfer function in dB.

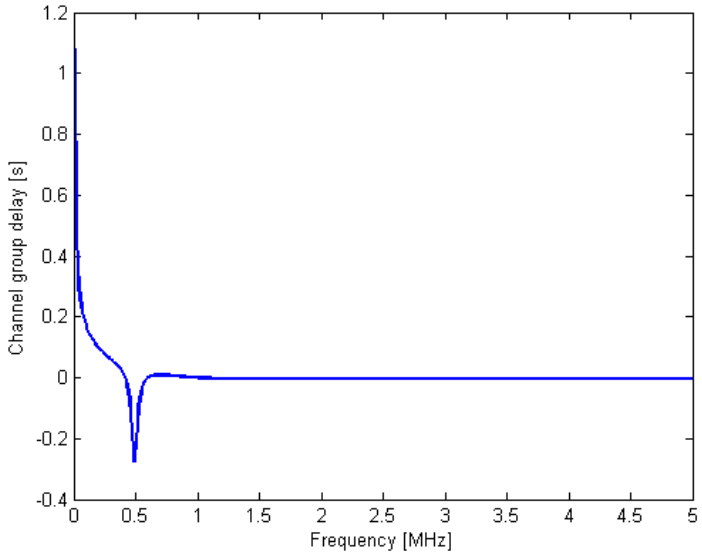

Figure 3.3: Channel group delay.

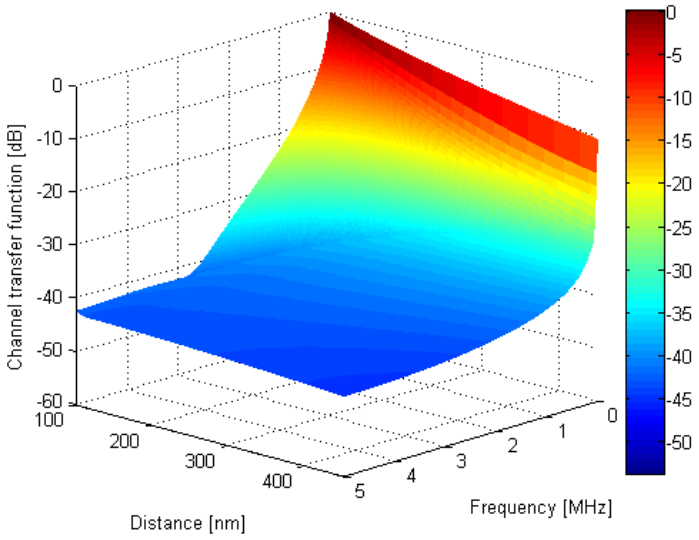

Figure 3.4: Magnitude of the normalized channel transfer function in dB as a function of the transmission distance.

frequency and the transmission distance. The transmission distance ranges from 100 to 450 nm. As expected, the channel attenuation increases both with the increase in frequency and in transmission distance. The channel group delay also increases with the the distance from the transmitter, and is nearly zero for frequencies higher than a few hundreds of kHz.

3.4 Communication Metrics

Eq. (3.1) can also be interpreted as the *pulse equation*, since it shows the evolution of a molecular pulse in space and time. Considering the pulse-based modulation scheme introduced in Section 3.2, an alternative path to explore the characteristics of the molecular channel is to directly analyze the pulse equation. With this purpose, we consider several metrics that will enable the assessment of the communication performance in this scenario. We focus on three of them: the pulse delay, the pulse amplitude and the pulse width. First, we obtain analytical expressions for these metrics and validate them by simulation. Then, we compare the scalability of these metrics with their equivalent in a wireless electromagnetic channel.

3.4.1 Pulse Delay

In order to find the pulse delay, we compute the time instant for which the pulse equation reaches its global maximum. As we observe in Fig. 3.1, this function has only one local maximum, which is also its global maximum. We can therefore compute the position of this maximum by taking the time derivative of the function and finding the time instant at which it is equal to zero:

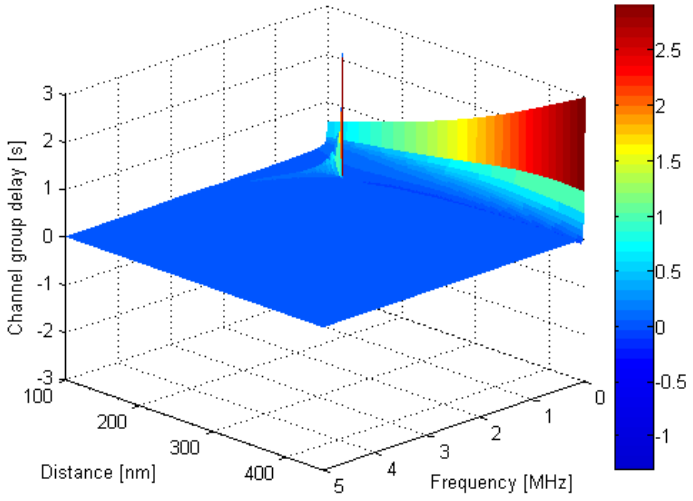

Figure 3.5: Channel group delay as a function of the transmission distance.

$$\frac{dc(r,t)}{dt} = \frac{d}{dt}\frac{Qe^{-r^2/4Dt}}{(4\pi Dt)^{3/2}} = 0 \tag{3.2}$$

From this equation, by isolating the variable t we can obtain the time at which the pulse has its maximum t_d. This time can be interpreted as the pulse delay:

$$t_d = \frac{r^2}{6D} \tag{3.3}$$

In order to validate this result, we simulate the transmission of a 10^7 molecule pulse using *NanoSim*. The diffusion coefficient is set to $D = 1$ nm^2/ns and the local molecular concentration is measured at distances from 100 to 450 nm, at intervals of 50 nm. We will use these same conditions throughout this work, unless otherwise stated. Fig. 3.6 shows a comparison between the analytical expression of the pulse delay (dashed line) and the averaged results obtained with *NanoSim* after 30 simulation runs with 95% confidence intervals.

3.4.2 Pulse Amplitude

It is also worth investigating the variation of the pulse amplitude over space, which may be interpreted as the channel attenuation. We obtain this amplitude by evaluating the pulse equation at the time instant at which the pulse reaches its maximum value, which we have previously found in Eq. (3.3):

$$c_{max} = c(r,t)|_{t=t_d} = \left(\frac{3}{2\pi e}\right)^{3/2}\frac{Q}{r^3} \tag{3.4}$$

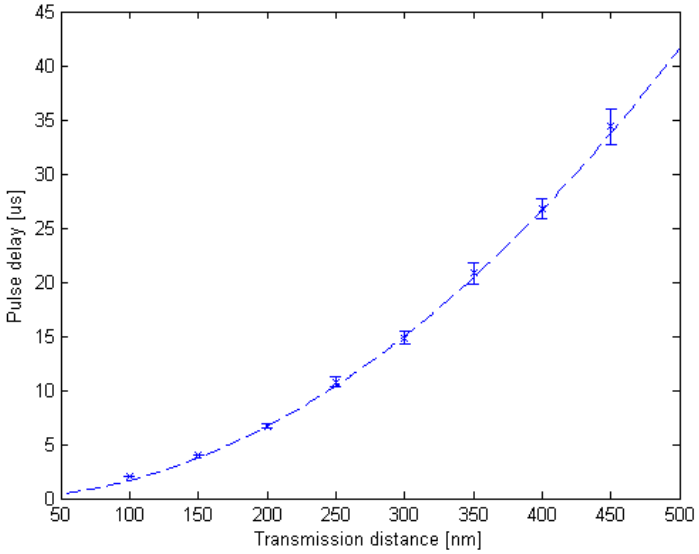

Figure 3.6: Plot of the pulse delay as a function of the transmission distance. The dashed line corresponds to the analytical expression, and the crosses show the simulation results with 95% confidence intervals.

As done in the previous section, we validate this result by means of simulation. Considering a pulse transmission under the same conditions used to validate the pulse delay, we measure the pulse amplitude as a function of the transmission distance. Fig. 3.7 shows a log-log plot that compares the analytical expression (dashed line) with the simulation results with 95% confidence intervals, which confirms the correctness of Eq. (3.4).

3.4.3 Pulse Width

Another important metric is the pulse width, since it will be the main constraint on the achievable bandwidth. As it is usually done in electromagnetic communication, we compute the pulse width at the 50% level, i.e., the time interval at which the pulse has an amplitude greater than half of its maximum value:

$$c(r,t) = \frac{Q}{(4\pi Dt)^{3/2}} e^{-r^2/4Dt} = \frac{c_{max}}{2} = \frac{1}{2}\left(\frac{3}{2\pi e}\right)^{3/2} \frac{Q}{r^3} \tag{3.5}$$

We obtain the following expression by isolating the time variable:

$$t = -\frac{r^2}{6DW\left(-\frac{1}{2^{2/3}e}\right)} \tag{3.6}$$

where W is the Lambert W function [16]. This equation has two solutions, corresponding to the two time instants at which the pulse amplitude is equal to half of its maximum value. These instants are given by:

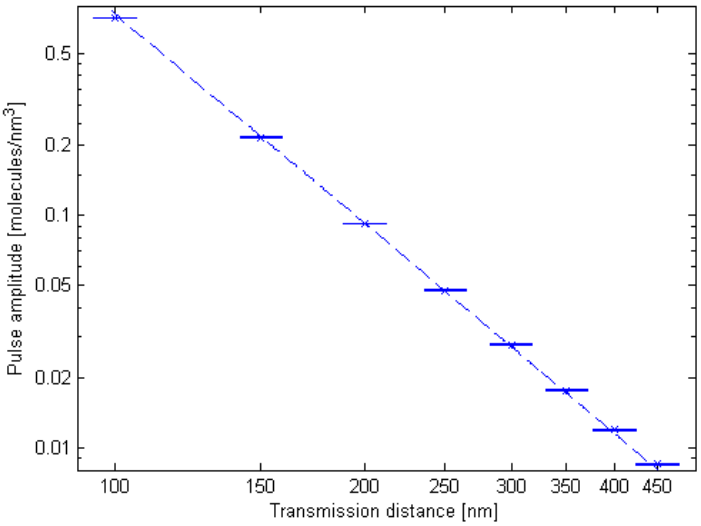

Figure 3.7: Log-log plot of the pulse amplitude as a function of the transmission distance. The dashed line corresponds to the analytical expression, and the crosses show the simulation results with 95% confidence intervals.

$$t_1 = \frac{0.0728}{D} r^2 \qquad t_2 = \frac{0.5229}{D} r^2 \tag{3.7}$$

Finally, we can obtain the expression of the pulse width t_w by subtracting these two instants:

$$t_w = t_2 - t_1 = \frac{0.4501}{D} r^2 \tag{3.8}$$

As before, we validate the obtained expression with *NanoSim*, using the same parameters as in the previous sections. Fig. 3.8 shows that the simulation results are close to the values of the analytical expression, which confirms the validity of Eq. (3.8).

3.4.4 Molecular vs Wireless EM Channel Comparison

It is worth comparing the communication performance metrics previously found for a diffusion-based molecular communication channel to their equivalent in a wireless electromagnetic (EM) communication channel. In the molecular channel, as we observe in Eq. (3.3), the pulse delay is proportional to the square of the transmission distance: $t_d = \Theta(r^2)$. This is due to the peculiarities of the Brownian motion underlying the diffusion process, which is fundamentally different from the wave propagation observed in EM communication. In the latter case, the propagation delay is equal to the transmission distance divided by the wave propagation speed: $t_d = \Theta(r)$.

Eq. (3.4) shows that the amplitude of a molecular pulse is inversely proportional to the third power of the transmission distance, i.e., $c_{max} = \Theta(1/r^3)$.

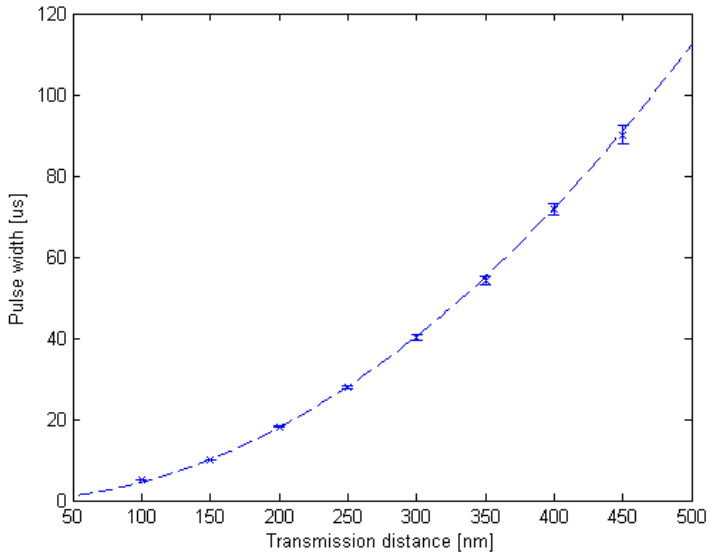

Figure 3.8: Plot of the pulse width as a function of the transmission distance. The dashed line corresponds to the analytical expression, and the crosses show the simulation results with 95% confidence intervals.

This dependence shows again a difference with respect to the behavior of waves in wireless EM communication, for which, according to the free-space path loss formula $A = \left(\frac{4\pi r f}{c}\right)^2$, the pulse amplitude decreases proportionally to the square of the transmission distance.

Finally, according to Eq. (3.8), the dependence of the pulse width on the transmission distance is $t_w = \Theta\left(r^2\right)$. Again, there is a clear difference with the traditional EM channel, for which the pulse width is independent from the transmission distance: $t_w = \Theta(1)$. Also, the behavior of the molecular channel differs from that observed in optical communication, where chromatic dispersion causes the pulse width to increase proportionally to the transmission distance ($t_w = \Theta(r)$), at a slower rate than in the molecular channel.

In the following table, we summarize these comparisons between the scalability of communication metrics in the molecular channel and the wireless electromagnetic channel:

Metric	**EM channel**	**Molecular channel**
Pulse delay	$\Theta\left(r\right)$	$\Theta\left(r^2\right)$
Pulse amplitude	$\Theta\left(1/r^2\right)$	$\Theta\left(1/r^3\right)$
Pulse width	$\Theta\left(1\right)$	$\Theta\left(r^2\right)$

3.5 Achievable Bandwidth

The pulse width expression, described in Eq. (3.8), allows us to obtain an estimate on the achievable bandwidth of the pulse-based modulation scheme.

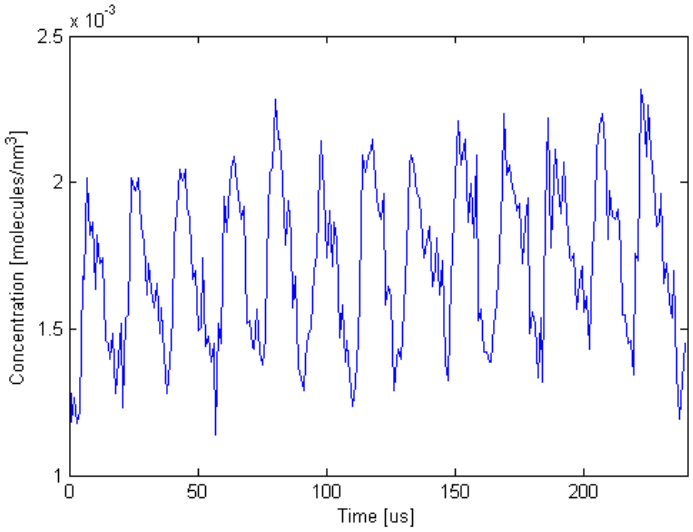

Figure 3.9: Concentration measured by the receiver when a train of pulses is transmitted from a distance of 200 nm. The interval between pulses is equal to the pulse width at the receiver location.

Let us consider the case where a nanomachine needs to transmit a bit stream. With this purpose, it may send a train of pulses by using different molecule types to represent bits '0' and '1', respectively. In this case, the minimum separation between the transmitted pulses needs to be approximately equal to the pulse width at the receiver, so that pulses can be correctly distinguished and the information can be decoded (assuming that the transmitter and receiver are synchronized). The achievable bandwidth in this scenario is thus approximately equal to the inverse of the pulse width at the receiver location.

The transmitter is able to compute the pulse width at the receiver by using Eq. (3.8) and it can set the interval between the transmitted pulses accordingly. For example, for a transmission distance of 200 nm, the received pulse width will be of 18 µs. Fig. 3.9 represents the received signal when a train of pulses is transmitted by a nanomachine located 200 nm away with an interval between pulses equal to the pulse width at the receiver (18 µs). The simulation results show a stream of distinguishable pulses and thus confirm that the transmitted signal can be correctly decoded by the receiver.

3.6 Multiple Transmitters

In order to demonstrate the feasibility of a scenario where multiple nanomachines are transmitting simultaneously, we perform a simulation where two transmitters emit a pulse of molecules at the same time instant. Fig. 3.10 shows the concentration measured by a receiver in this scenario. The transmitter nanomachines are located at a distance of 300 and 400 nm, respectively, and they use different molecule types in order to avoid the collision of the transmitted pulses. Since the transmitted molecules do not interact, the pulses are

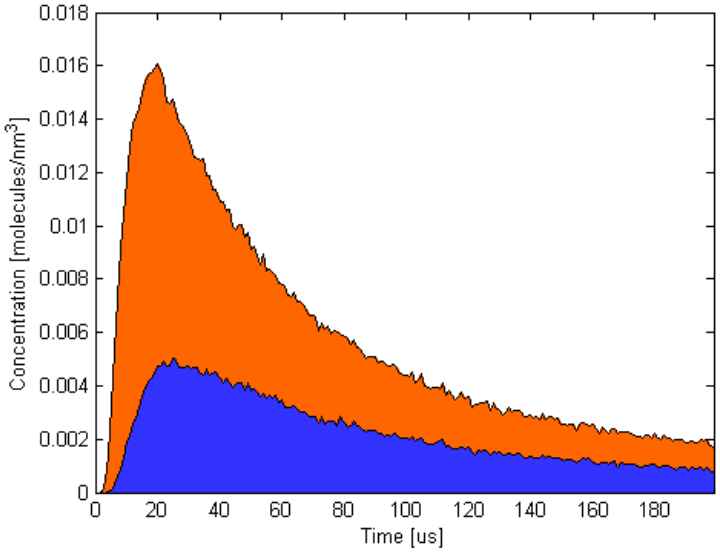

Figure 3.10: Concentration measured by the receiver when two transmitters simultaneously emit a molecular pulse. Transmitter 1 (orange) is located at a distance of 300 nm, and transmitter 2 (blue) at 400 nm.

orthogonal and they can be successfully decoded by the receiver.

Chapter 4

NanoSim: A Simulation Framework for Diffusion-based Molecular Communication

4.1 Introduction

Several authors have developed analytical models of diffusion-based molecular communication [50, 27]. In order to validate them, either an experimental study or simulations are needed. Despite recent advances in synthetic biology, an experimental setup of molecular communication is still very challenging to build, so simulation seems the most feasible choice nowadays. A simulator would allow to recreate a molecular communication environment and measure the relevant metrics to evaluate its performance, such as channel attenuation, delay and capacity. The simulator outputs can be then compared with the results from the analytical models in order to assess the validity of the models.

Some authors have obtained simulation results, but restricted to very simple scenarios where the transmitter releases a single molecule [39]. Other simulators are based on Fick's laws of diffusion [32], making it impossible to simulate collisions among particles (collective diffusion) or observe effects like noise due to the diffusion itself. Therefore, to the best of our knowledge, a realistic simulation tool which allows to validate the existing theoretical models and to create novel, more accurate models is currently missing.

With the objective of filling this gap, we present next a brief overview of the simulation framework *NanoSim* [1], which allows the molecule-by-molecule simulation of diffusion-based molecular networks. The benefits of *NanoSim* include the validation of existing channel models for molecular communication and the evaluation of novel modulation schemes. In particular, in Section 3.4, we used *NanoSim* to validate our obtained analytical results.

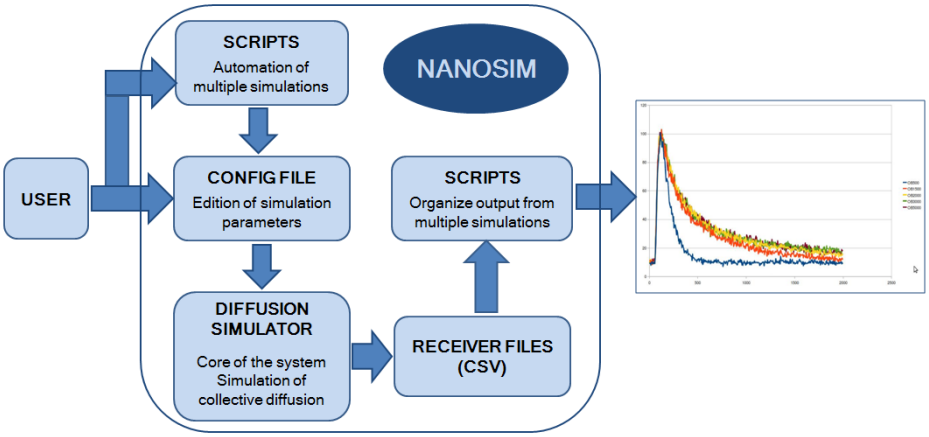

Figure 4.1: Block diagram of *NanoSim*

4.2 Simulator Architecture

The simulated scenario can be described as a group of nanomachines which communicate through molecular diffusion in a 3-dimensional fluid medium. Each transmitter is modeled as a punctual nanomachine with a fixed location. Transmitters encode the information by releasing molecules into the medium with a user-specified pattern. The emitted molecules move according to Brownian motion, as a result of collisions with the smaller fluid molecules. Finally, receivers are modeled as spherical nanomachines which are able to count the number of molecules in a surrounding volume, thus estimating the local concentration. From this measurement, the transmitted information can be decoded.

Figure 4.1 shows a block diagram of the steps needed to run a simulation. First, the user specifies the simulation parameters in a configuration file. A set of scripts allows the user to run multiple simulations automatically. Next, the diffusion simulator takes these files as input and generates an output file for each receiver. Finally, another set of scripts may be used to plot the simulation results.

4.2.1 Transmitter and Receiver Models

The transmitter is defined by its location in the simulation space and its size, which determines its influence area. Every transmitter also has an associated waveform, which modulates its particle release pattern. There are a number of predefined waveforms, such as a square pulse, a Gaussian pulse or a pulse wave, amongst others. Moreover, the user may define a custom waveform to be used by the transmitter.

The receiver can be modeled as a sphere or cube which is able to measure the instantaneous number of molecules within its detection range, from which the local concentration can be estimated. This model is inspired by the ligand-receptor binding mechanism found in nature [55]. Many receiver pa-

rameters are customizable. For instance, after the receiver has measured a set of particles, it can either absorb them or be completely transparent to them.

NanoSim also allows the user to place multiple transmitters and receivers in the simulation field. The user just needs to define the characteristics of each transmitter and receiver, namely, its position, shape and size, which can be different for each of them. This will allow the study of several communication aspects, such as the feasibility of broadcast molecular communication, or the nature of interferences when more than one transmitter emits at the same time.

4.2.2 Particle Model

We model the particles as spheres. The main reason for this choice is the simplicity of the collision detection algorithm for spheres. The diffusion of the emitted particles takes place as a result of the collisions between particles and the fluid molecules. It would be computationally infeasible to model each of these collisions individually, since the number of collisions between each particle and the fluid molecules is in the order of 10^{20} per second [49]. Fortunately, the seemingly random movement of the suspended particles caused by collisions between the particles and the smaller fluid molecules can be modeled mathematically as Brownian motion [40]. Brownian motion allows to statistically calculate the movement of each particle, which behaves as a Gaussian random variable with zero mean and whose root mean square displacement in each dimension after a time t is $\sqrt{2Dt}$, where D is the diffusion coefficient of the medium [20].

The high-level effect of the particles moving with a Brownian pattern is their diffusion throughout the medium. Fick's laws [48] model the diffusion which results from the collisions between the particles and fluid molecules. However, they do not take into account the influence of collisions among the particles themselves, and thus are only valid when the particle concentration is low.

In order to simulate diffusion environments with a high background concentration (known as collective diffusion [7]), *NanoSim* needs to account for collisions among particles and the particles inertia. For simplicity, we consider that all collisions are elastic (i.e., the total kinetic energy is conserved). Since the particles are modeled as spheres, *NanoSim* can efficiently detect and compute the collisions among them. Since collisions among particles only have an effect on their diffusion when the concentration is high, collisions may be disabled in order to further increase the speed of the simulation.

4.2.3 Simulation Space

NanoSim can be configured to generate both 2-dimensional and 3-dimensional simulation spaces. One of its parameters is the initial particle concentration in the medium. If it is zero, an unbounded space can be simulated. However, if the initial particle concentration is greater than zero, the simulation space needs to be bounded (otherwise the number of particles would be infinite).

When a bounded space is simulated, a cuboidal simulation space is assumed. We considered several alternatives to implement the simulation space:

1. We place hard boundaries at the edges of the simulation space. When a particle reaches one of these boundaries, it rebounds.

2. The space has transparent boundaries; whenever a particle crosses them and moves outside the simulation field, it disappears.

3. The space has transparent boundaries; whenever a particle reaches a boundary, it reappears in the other side of the simulation area, as in a torus-shaped scenario.

We decided to implement the first alternative, which we consider the most realistic in prospective applications of molecular communication. For example, in a set of communicating nanomachines located in a blood vessel, whenever a particle collides with the vessel wall (known as *tunica intima*), it will rebound.

The particles released by transmitters will increase the background concentration over time, which may be unrealistic in some scenarios. For such cases, *NanoSim* includes an optional mechanism which simulates an infinite space by letting some particles disappear at the system bounds, according to the laws of diffusion.

Moreover, objects can also be set within the scenario in order to simulate obstacles between the transmitters and receivers. This will allow recreating, for example, a scenario where a group of bacteria is crossing the medium and it obstructs the way between transmitters and receivers.

4.3 Simulation Results

In order to illustrate the capabilities of the simulator, we performed several simple simulations in a 2-dimensional space with a circular transmitter and receiver of 100 nm in radius. Table 4.1 contains the values of the parameters used. Fig. 4.2 shows the transmission of a Gaussian pulse consisting of 10^6 molecules, and the received signal, defined as the number of particles detected by a receiver as a function of time, at 500 and 1000 nm from the transmitter location, respectively. We observe that the molecular channel alters the shape of the pulse. As the transmission distance increases, the received pulse is lower, wider and has a longer tail, due to the effect of diffusion.

In Fig. 4.3, we see the molecular channel response to a square pulse. In this case, the distortion of the pulse shape by the molecular channel is even more pronounced. At a distance of 1000 nm, the square pulse is indistinguishable from the Gaussian pulse. This suggests that, in this environment, a modulation based on Gaussian pulses might be more suitable than one based on square pulses.

Parameter	**Value**
Time step	10 µs
Simulation time	5 ms
Transmitter radius	100 nm
Receiver radius	100 nm
Particle radius	0.2 nm
Number of particles released	10^6
Diffusion constant	0.896 nm^2/ns

Table 4.1: Parameters used in the simulations

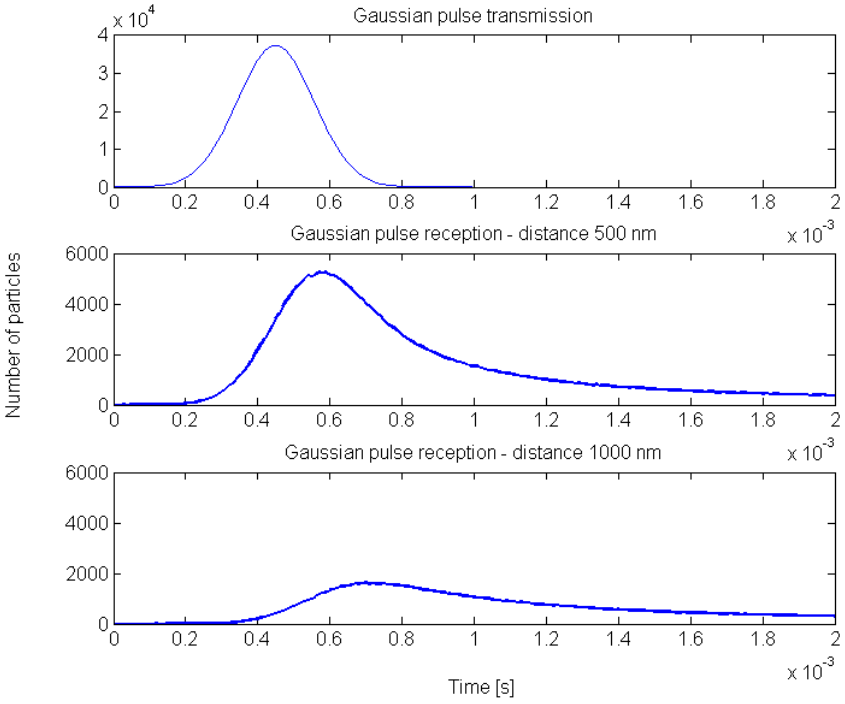

Figure 4.2: Transmission of a Gaussian pulse

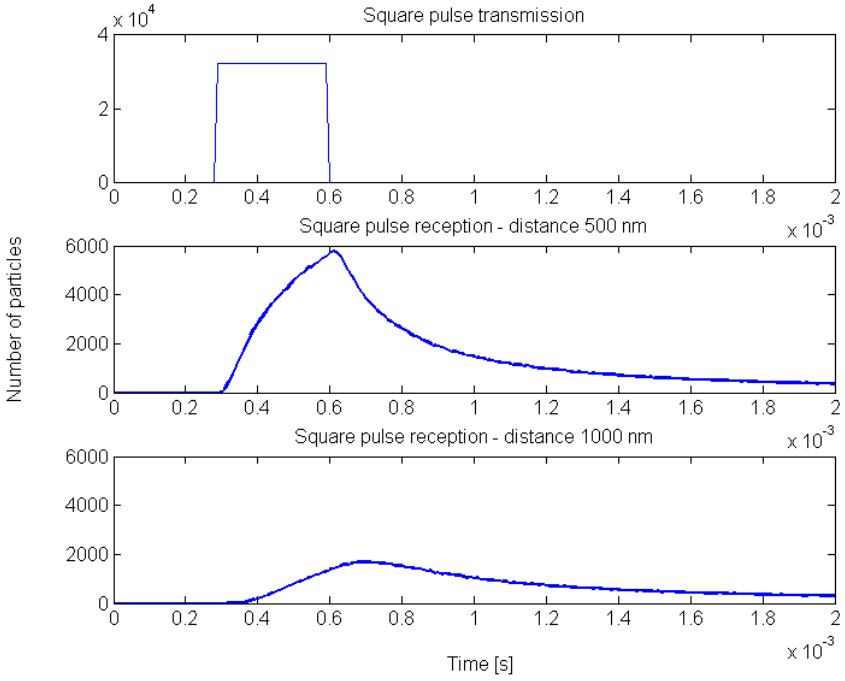

Figure 4.3: Transmission of a square pulse

Chapter 5

Conclusions and future work

5.1 Conclusions

Nanonetworks, the interconnection of nanomachines, will greatly expand the range of applications of nanotechnology, bringing new opportunities in diverse fields. Following preliminary studies on techniques to enable communications at the nanoscale, two paradigms that promise the realization of nanonetworks have emerged: molecular communication and nano-electromagnetic communication.

A key question then arises: do nanonetworks have the potential of becoming a *reality* or will they remain in the realm of *science fiction*? One way to obtain the answer to this question is to study the scalability of the performance metrics in a communication network, such as the throughput, the transmission delay and the energy consumption, when the network size is reduced to the nanoscale.

In this work, we lay the foundations of a scalability theory for nanonetworks, which will allow to determine the *feasibility* of nanonetworks. In order to find how the performance metrics of the network scale, the communication channel first needs to be characterized.

In the case of nano-electromagnetic communication, we analyze a recently-presented channel model [37] based on the use of graphene-based nanoantennas which radiate electromagnetic waves at the terahertz band. We identify several *quantum effects* arising from the use of graphene-based nanoantennas, which do not appear when traditional metallic antennas are employed. By finding how these effects impact communication at the nanoscale, we obtain the scalability of the nano-electromagnetic channel capacity when the network dimensions shrink. Our quantitative results show that the channel capacity scales better when quantum effects are present. Finally, we derive guidelines regarding *how* network parameters, such as the transmission distance or the transmitted power, need to scale in order to keep the network feasible.

In molecular communication, we concentrate in a scenario of short-range molecular signaling governed by Fick's laws of diffusion. For this scenario, a physical channel model that allows the development of a scalability theory is missing. Therefore, the diffusion-based molecular channel needs to be char-

acterized in order to lay the groundwork for a scalability theory. With this purpose, we follow two complementary approaches. First, we obtain the impulse response, the transfer function and the group delay of the molecular channel. Second, we propose a pulse-based modulation scheme and, based on this scheme, we derive analytical expressions for the most relevant performance metrics from the communication standpoint: the pulse delay, the pulse amplitude and the pulse width. We then validate these results by means of simulation. Last, we show the differences in the scalability of the obtained metrics with respect to their equivalent in wireless electromagnetic communication.

Motivated by the need to validate the analytical expressions for the previously obtained performance metrics, we have designed *NanoSim*, a physical simulation framework for diffusion-based molecular communication. We think that *NanoSim* will prove an essential tool to design and evaluate protocols, modulations, resource management schemes and a novel network architecture for molecular nanonetworks.

In conclusion, we consider that the results of this thesis provide interesting insights which may serve designers as a guide to implement future nanonetworks, and lay the foundations of a scalability theory for nanonetworks.

5.2 Future work

Nanonetworking is a vast research field whose exploration began only a few years ago [4]. This thesis contains just the foundations of a scalability theory of nanonetworks; thus, the possibilities of extending this work are almost endless. We outline next just a few of them.

A scalability theory of nano-electromagnetic communication needs to consider how all the relevant performance metrics scale. In this thesis, we focused on the nanoantenna and evaluated the scalability of the channel capacity, but studying other metrics is no less important. For instance, aspects such as the memory requirements, the energy consumption and the transmission range of nanomachines will be of utmost importance when designing nanonetworks. In order to find how these metrics scale, our scalability analysis must be extended to include all the nanodevices that make up the nanomachine, such as the nano-battery, the nano-processor, the nano-memory and the nano-transceiver. A complete scalability theory should explain how the size and the performance of each of these nanodevices will scale in nanonetworks.

Our study of the molecular communication scenario only considers molecular signaling, one of the proposed techniques for the short range (nm to µm). Furthermore, the analyzed performance metrics are only evaluated for a particular modulation scheme. Our work should be thus generalized to include other modulations, scenarios and communication techniques, as well as additional performance metrics. However, we expect the development of a unified scalability theory for molecular communication to be a challenging task, due to the broad variety of communication scenarios for which a channel model has not been developed to date.

Finally, the simulation framework *NanoSim* is just a first attempt to recreate a scenario of diffusion-based molecular communication. It can be extended in several directions, such as considering additional effects (e.g., electrostatic charges) in order to provide a closer approximation to reality, and improving its scalability in complex scenarios.

Appendix A

Derived publications and theses

A.1 Publications derived from this thesis

- Ignacio Llatser, Albert Cabellos-Aparicio, Eduard Alarcón, Josep Miquel Jornet, and Ian F. Akyildiz. Scalability of the Channel Capacity of Electromagnetic Nanonetworks. To be submitted to *IEEE Transactions on Wireless Communications*.

- Ignacio Llatser, Albert Cabellos-Aparicio, Eduard Alarcón, and Massimiliano Pierobon. Diffusion-based Channel Characterization in Molecular Nanonetworks. Submitted to the *1st IEEE International Workshop on Molecular and Nano Scale Communication (MoNaCom)*, organized in conjunction with *IEEE Infocom 2011*.

- Nora Garralda, Ignacio Llatser, Albert Cabellos-Aparicio, Eduard Alarcón, and Massimiliano Pierobon. Simulation-based Evaluation of the Diffusion-based Physical Channel in Molecular Nanonetworks. Submitted to the *1st IEEE International Workshop on Molecular and Nano Scale Communication (MoNaCom)*, organized in conjunction with *IEEE Infocom 2011*.

- Ignacio Llatser, Iñaki Pascual, Nora Garralda, Albert Cabellos-Aparicio, Massimiliano Pierobon, Eduard Alarcón, and Josep Solé-Pareta. NanoSim: A Simulation Framework for Diffusion-based Molecular Communication. In preparation.

A.2 Supervised master theses

- Nora Garralda. Simulation-based Evaluation of the Diffusion-based Physical Channel in Molecular Nanonetworks. Supervised by Albert Cabellos-Aparicio and Ignacio Llatser, to be defended in February 2011.

- Iñaki Pascual. NanoSim: Simulation Tool for Diffusion-based Molecular Comunication in Nanonetworks. Supervised by Albert Cabellos-Aparicio and Ignacio Llatser, to be defended in June 2011.

Bibliography

[1] Nanonetworking Center in Catalunya. `http://www.n3cat.upc.edu`.

[2] S. Abadal. *Automata Modeling of Quorum Sensing for Nanocommunication Networks*. PhD thesis, Technical University of Catalonia, 2010.

[3] J. Ahn and B. Krishnamachari. Fundamental Scaling Laws for Energy-Efficient Storage. In *ACM International Symposium on Mobile Ad Hoc Networking and Computing (MobiHoc)*, pages 334–343, Florence, 2006.

[4] I. F. Akyildiz, F. Brunetti, and C. Blázquez. Nanonetworks: A new communication paradigm. *Computer Networks*, 52(12):2260–2279, 2008.

[5] I. F. Akyildiz and J. Jornet. The Internet of nano-things. *IEEE Wireless Communications*, 17(6):58–63, 2010.

[6] I. F. Akyildiz and J. M. Jornet. Electromagnetic wireless nanosensor networks. *Nano Communication Networks*, 1(1):3–19, May 2010.

[7] T. Ala-Nissila, R. Ferrando, and S. Ying. Collective and single particle diffusion on surfaces. *Advances in Physics*, 51(3):949–1078, 2002.

[8] D. Arifler. Capacity Analysis of a Diffusion-Based Short-Range Molecular Nano-Communication Channel. *Computer Networks*, In Press, Dec. 2010.

[9] B. Atakan and O. B. Akan. On molecular multiple-access, broadcast, and relay channels in nanonetworks. In *International Conference on Bio-Inspired Models of Network, Information and Computing Sytems*, 2008.

[10] P. Avouris, Z. Chen, and V. Perebeinos. Carbon-based electronics. *Nature nanotechnology*, 2(10):605–15, Oct. 2007.

[11] M. J. Berridge. The AM and FM of calcium signaling. *Nature*, 386(6627):759–760, Feb. 1997.

[12] W. H. Bossert and E. O. Wilson. The analysis of olfactory communication among animals. *Journal of theoretical biology*, 5(3):443–69, Nov. 1963.

[13] P. J. Burke, S. Li, and Z. Yu. Quantitative theory of nanowire and nanotube antenna performance. *IEEE Transactions on Nanotechnology*, 5(4):314–334, 2006.

[14] E. Carafoli. Calcium signaling: a tale for all seasons. *Proc. of the National Academy of Sciences of the United States of America*, 99(3):1115–22, Feb. 2002.

[15] D. E. Clapham. Calcium signaling. *Cell*, 131(6):1047–58, Dec. 2007.

[16] R. M. Corless, G. H. Gonnet, D. E. G. Hare, D. J. Jeffrey, and D. E. Knuth. On the Lambert W function. *Advances in Computational Mathematics*, 5(1):329–359, Dec. 1996.

[17] R. Dennard, F. Gaensslen, V. Rideout, E. Bassous, and A. Leblanc. Design of Ion-implanted MOSFET's with Very Small Physical Dimensions. *IEEE Journal of Solid-State Circuits*, SC-9(5):256–268, Apr. 1974.

[18] B. S. Donahue and R. Abercrombie. Free diffusion coefficient of ionic calcium in cytoplasm. *Cell Calcium*, 8(6):437–448, 1987.

[19] K. E. Drexler. *Nanosystems: Molecular machinery, manufacturing, and computation*. Wiley, 1992.

[20] A. Einstein. *Investigations on the theory of the brownian movement*. 1915.

[21] C. Falconi, A. Damico, and Z. Wang. Wireless Joule nanoheaters. *Sensors and Actuators B: Chemical*, 127(1):54–62, Oct. 2007.

[22] R. Fernández-Pacheco, C. Marquina, J. Gabriel Valdivia, M. Gutiérrez, M. Soledad Romero, R. Cornudella, A. Laborda, A. Viloria, T. Higuera, A. Garcia, J. A. García de Jalón, and M. Ricardo Ibarra. Magnetic nanoparticles for local drug delivery using magnetic implants. *Journal of Magnetism and Magnetic Materials*, 311(1):318–322, Apr. 2007.

[23] D. Foty. Perspectives on scaling theory and CMOS technology - understanding the past, present, and future. In *IEEE International Conference on Electronics, Circuits and Systems*, pages 631–637, 2004.

[24] R. A. Freitas. Nanotechnology, nanomedicine and nanosurgery. *International Journal of Surgery*, 3(4):243–6, Jan. 2005.

[25] H. E. Gamal. On the Scaling Laws of Dense Wireless Sensor Networks : The Data Gathering Channel. *IEEE Transactions on Information Theory*, 51(3):1229–1234, 2005.

[26] A. K. Geim and K. S. Novoselov. The rise of graphene. *Nature materials*, 6(3):183–91, Mar. 2007.

[27] A. Goldbeter, G. Dupont, and M. J. Berridge. Minimal model for signal-induced Ca2+ oscillations and for their frequency encoding through protein phosphorylation. *Proc. of the National Academy of Sciences of the United States of America*, 87(4):1461–5, Feb. 1990.

[28] A. Goldsmith. *Wireless Communications*. Cambridge University Press, 2005.

[29] R. M. Goody and Y. L. Yung. *Atmospheric Radiation: Theoretical basis*. Oxford University Press, 2nd edition, 1989.

[30] M. Gregori, I. Llatser, A. Cabellos-Aparicio, and E. Alarcón. Physical channel characterization for medium-range nano-networks using flagellated bacteria. *Computer Networks*, in press, Oct. 2010.

[31] M. Gregori, I. Llatser, A. Cabellos-Aparicio, and E. Alarcón. Physical channel characterization for medium-range nanonetworks using catalytic nanomotors. *Nano Communication Networks*, 1(2):102–107, June 2010.

[32] E. Gul, B. Atakan, and O. B. Akan. NanoNS: A nanoscale network simulator framework for molecular communications. *Nano Communication Networks*, 1(2):138–156, June 2010.

[33] P. Gupta and P. R. Kumar. The capacity of wireless networks. *IEEE Transactions on information theory*, 46(2):388–404, 2000.

[34] J. Han, J. Fu, and R. B. Schoch. Molecular sieving using nanofilters: past, present and future. *Lab on a chip*, 8(1):23–33, Jan. 2008.

[35] G. Hanson. Fundamental transmitting properties of carbon nanotube antennas. *IEEE Transactions on Antennas and Propagation*, 53(11):3426–3435, Nov. 2005.

[36] A. Jordan, P. Wust, R. Scholz, B. Tesche, H. Fähling, T. Mitrovics, T. Vogl, J. Cervós-Navarro, and R. Felix. Cellular uptake of magnetic fluid particles and their effects on human adenocarcinoma cells exposed to AC magnetic fields in vitro. *International journal of hyperthermia*, 12(6):705–22, 1996.

[37] J. M. Jornet and I. F. Akyildiz. Channel Capacity of Electromagnetic Nanonetworks in the Terahertz Band. In *IEEE International Conference in Communications*, Cape Town, 2010.

[38] J. M. Jornet and I. F. Akyildiz. Graphene-Based Nano-Antennas for Electromagnetic Nanocommunications in the Terahertz Band. In *European Conference on Antennas and Propagation*, Barcelona, 2010.

[39] S. Kadloor and R. Adve. A Framework to Study the Molecular Communication System. In *International Conference on Computer Communications and Networks*, San Francisco, 2009.

[40] I. Karatzas and S. Shreve. *Brownian motion and stochastic calculus*. Springer, 1991.

[41] O. Lévêque and I. E. Telatar. Information-Theoretic Upper Bounds on the Capacity of Large Extended Ad Hoc Wireless Networks. *IEEE Transactions on Information Theory*, 51(3):858–865, 2005.

[42] C. Li, E. Thostenson, and T. Chou. Sensors and actuators based on carbon nanotubes and their composites: A review. *Composites Science and Technology*, 68(6):1227–1249, May 2008.

[43] J.-Q. Liu. Molecular informatics of nano-communication based on cells: A brief survey. *Nano Communication Networks*, 1(2):118–125, June 2010.

[44] S. Luryi, J. Xu, and A. Zaslavsky. *Scaling Limits of Silicon CMOS and Non-silicon opportunities*, pages 203–211. Wiley, 2007.

[45] M. E. Moses, S. Forrest, A. L. Davis, M. A. Lodder, and J. H. Brown. Scaling theory for information networks. *Journal of the Royal Society Interface*, 5(29):1469–1480, 2008.

[46] T. Nakano, T. Suda, M. J. Moore, R. Egashira, A. Enomoto, and K. Arima. Molecular communication for nanomachines using intercellular calcium signaling. In *IEEE Conference on Nanotechnology*, number July, pages 632–635, 2005.

[47] L. Parcerisa and I. F. Akyildiz. Molecular communication options for long range nanonetworks. *Computer Networks*, 53(16):2753–2766, 2009.

[48] J. Philibert. One and a Half Century of Diffusion: Fick, Einstein, before and beyond. *Diffusion Fundamentals*, 4(6):1–19, 2006.

[49] J. Piasecki. Centenary of Marian Smoluchowski's Theory of Brownian Motion. *Acta Physica Polonica Series B*, 38(5):1623, 2007.

[50] M. Pierobon and I. F. Akyildiz. A physical end-to-end model for molecular communication in nanonetworks. *IEEE Journal on Selected Areas in Communications*, 28(4):602–611, 2010.

[51] M. Pierobon and I. F. Akyildiz. Information Capacity of Diffusion-based Molecular Communication in Nanonetworks. In *IEEE Infocom Miniconference*, Shanghai, 2011.

[52] R. Piesiewicz, T. Kleine-Ostmann, N. Krumbholz, D. Mittleman, M. Koch, J. Schoebei, and T. Kurner. Short-Range Ultra-Broadband Terahertz Communications: Concepts and Perspectives. *IEEE Antennas and Propagation Magazine*, 49(6):24–39, Dec. 2007.

[53] C. M. J. Pieterse and M. Dicke. Plant interactions with microbes and insects: from molecular mechanisms to ecology. *Trends in plant science*, 12(12):564–9, Dec. 2007.

[54] J. Riu, A. Maroto, and F. X. Rius. Nanosensors in environmental analysis. *Talanta*, 69(2):288–301, Apr. 2006.

[55] J. P. Rospars, V. Krivan, and P. Lánský. Perireceptor and receptor events in olfaction. Comparison of concentration and flux detectors: a modeling study. *Chemical senses*, 25(3):293–311, June 2000.

[56] L. Rothman, I. Gordon, a. Barbe, D. Benner, P. Bernath, M. Birk, V. Boudon, L. Brown, a. Campargue, and J.-P. Champion. The HITRAN 2008 molecular spectroscopic database. *Journal of Quantitative Spectroscopy and Radiative Transfer*, 110(9-10):533–572, June 2009.

[57] C. E. Shannon. The mathematical theory of communication. 1963. *The Bell System Technical Journal*, 27:379–423, 623–656, 1948.

[58] P. Tallury, A. Malhotra, L. M. Byrne, and S. Santra. Nanobioimaging and sensing of infectious diseases. *Advanced drug delivery reviews*, 62(4-5):424–37, Mar. 2010.

[59] T. S. Ursell. The Diffusion Equation. A Multi-dimensional Tutorial, 2007.

[60] F. Vullum and D. Teeters. Investigation of lithium battery nanoelectrode arrays and their component nanobatteries. *Journal of Power Sources*, 146(1-2):804–808, Aug. 2005.

[61] F. Walsh, S. Balasubramaniam, D. Botvich, and W. Donnelly. Review of communication mechanisms for biological Nano and MEMS devices. In *2nd Bio-Inspired Models of Network, Information and Computing Systems*, pages 307–312, Dec. 2007.

[62] Z. L. Wang. Towards Self-Powered Nanosystems: From Nanogenerators to Nanopiezotronics. *Advanced Functional Materials*, 18(22):3553–3567, Nov. 2008.

[63] M. Wautelet. Scaling laws in the macro- , micro- and nanoworlds. *European Journal of Physics*, 22(6):601–611, 2001.

[64] H.-Y. Yeh, M. V. Yates, W. Chen, and A. Mulchandani. Real-time molecular methods to detect infectious viruses. *Seminars in cell & developmental biology*, 20(1):49–54, Feb. 2009.